haematologica
Journal of the Ferrata Storti Foundation

# LNK/SH2B3 as a novel driver in juvenile myelomonocytic leukemia

by Astrid Wintering, Anna Hecht, Julia Meyer, Eric B. Wong, Juwita Hübner, Sydney Abelson, Kira Feldman, Vanessa E. Kennedy, Cheryl A.C. Peretz, Deborah L. French, Jean Ann Maguire, Chintan Jobaliya, Marta Rojas Vasquez, Sunil Desai, Robin Dulman, Eneida Nemecek, Hilary Haines, Mahmoud Hammad, Alaa El Haddad, Scott C. Kogan, Zied Abdullaev, Farid F. Chehab, Sarah K. Tasian, Catherine C. Smith, Mignon L. Loh, and Elliot Stieglitz

*Received: June 21, 2023.*
*Accepted: December 19, 2023.*

*Citation: Astrid Wintering, Anna Hecht, Julia Meyer, Eric B. Wong, Juwita Hübner, Sydney Abelson, Kira Feldman, Vanessa E. Kennedy, Cheryl A.C. Peretz, Deborah L. French, Jean Ann Maguire, Chintan Jobaliya, Marta Rojas Vasquez, Sunil Desai, Robin Dulman, Eneida Nemecek, Hilary Haines, Mahmoud Hammad, Alaa El Haddad, Scott C. Kogan, Zied Abdullaev, Farid F. Chehab, Sarah K. Tasian, Catherine C. Smith, Mignon L. Loh, and Elliot Stieglitz. LNK/SH2B3 as a novel driver in juvenile myelomonocytic leukemia. Haematologica. 2023 Dec 28. doi: 10.3324/haematol.2023.283776 [Epub ahead of print]*

# LNK/*SH2B3* as a novel driver in juvenile myelomonocytic leukemia

Astrid Wintering[1], Anna Hecht[2], Julia Meyer[1], Eric B. Wong[1], Juwita Hübner[1], Sydney Abelson[1], Kira Feldman[1], Vanessa E. Kennedy[3], Cheryl A.C. Peretz[1,4], Deborah L. French[5], Jean Ann Maguire[5], Chintan Jobaliya[5], Marta Rojas Vasquez[6], Sunil Desai[6], Robin Dulman[7], Eneida Nemecek[8], Hilary Haines[9], Mahmoud Hammad[10], Alaa El Haddad[10], Scott C. Kogan[11], Zied Abdullaev[12], Farid F. Chehab[13], Sarah K. Tasian[14,15], Catherine C. Smith[3,4], Mignon L. Loh[#16], Elliot Stieglitz[#1,4]

[1]Department of Pediatrics, Benioff Children's Hospitals, University of California San Francisco, San Francisco, CA 94158, USA
[2]Department of Hematology/Oncology, Klinikum Rechts der Isar, Technische Universität München, München, Germany
[3]Division of Hematology/Oncology, Department of Medicine, University of California San Francisco, San Francisco, CA 94158, USA
[4]Helen Diller Comprehensive Cancer Center, University of California San Francisco, San Francisco, CA 94158, USA
[5]Center for Cellular and Molecular Therapeutics, The Children's Hospital of Philadelphia, Philadelphia, PA 19104, USA
[6]Department of Pediatrics, University of Alberta, Edmonton, AB T6G 1C9, Canada
[7]Pediatric Hematology and Oncology, Pediatric Specialists of Virginia, Fairfax, VA 22031, USA
[8]OHSU Knight Cancer Institute, Oregon Health and Science University, Portland, OR 97239, USA
[9]Children's of Alabama, University of Alabama Hospital, Birmingham, AL 35233, USA
[10]National Cancer Institute, Cairo University, Cairo, Egypt
[11]Department of Laboratory Medicine, University of California San Francisco, San Francisco, CA 94158, USA
[12]Laboratory of Pathology, Center for Cancer Research, National Cancer Institute, National Institutes of Health, Bethesda, MD 20814, USA
[13]Institute for Human Genetics, University of California San Francisco, San Francisco, CA 94143, USA
[14]Division of Oncology and Center for Childhood Cancer Research, Children's Hospital of Philadelphia; Philadelphia, PA 19104, USA
[15]Department of Pediatrics and Abramson Cancer Center, University of Pennsylvania Perelman School of Medicine; Philadelphia, PA 19104, USA
[16]Ben Towne Center for Childhood Cancer Research, Seattle Children's Research Institute, and the Department of Pediatrics, Seattle Children's Hospital, University of Washington, Seattle, WA, 98105, USA

**Footnotes:** [#]M.L. and E.S. contributed equally as senior authors to this work.

**Corresponding Authors:**

Elliot Stieglitz

Email: elliot.stieglitz@ucsf.edu

Phone: +1 (415) 514-9389

Mignon Loh
Email: mignon.loh@seattlechildrens.org
Phone: +1 (206) 987-8050

**Running Title:***SH2B3* as a novel driver in JMML

**Word Count:**

Abstract: 185

Main text: 3360

**Figures:** 4

**Tables:** 2

**Supplemental Tables:** 5

**Supplemental Figures:** 4

**Acknowledgments:** The authors acknowledge the patients and their families for consenting to a JMML research study. We would like to thank Brian Lockhart and Dr. Gerald Wertheim at the Children's Hospital of Philadelphia for assistance with patient specimens.

**Funding:** This work was supported by National Institutes of Health, National Heart, Lung, and Blood Institute grant K08HL135434 (E.S.); National Institutes of Health, National Cancer Institute grants 1U54CA196519 (M.L.L., E.S.); 1R37CA266550 (M.L.L., E.S.); the Pediatric Cancer Research Foundation (E.S.); the Frank A. Campini Foundation (E.S.); the Leukemia and Lymphoma Society grant R6511-19 (M.L.L.); the Coco Laziridis Foundation for JMML Research (S.K.T.); and the German Cancer Aid (A.W.). S.K.T. is a Scholar of the Leukemia & Lymphoma Society and holds the Joshua Kahan Endowed Chair in Pediatric Leukemia Research at the Children's Hospital of Philadelphia. M.L.L. is the Aldarra Foundation, June and Bill Boeing, Founders, Endowed Chair of Pediatric Oncology.

**Authorship Contributions:** A.W. performed experiments, analyzed data, and wrote the manuscript; A.H. performed experiments, analyzed data, and edited the manuscript; J.M. performed experiments and bioinformatic analysis; F.C. helped with bioinformatic analysis; E.W., J.H., S.A., and K.F. performed experiments; V.E.K., C.A.C.P., D.L.F., C.J. and J.A.M. performed experiments and analyzed data; M.R.V.,

S.D., R.D., E.N., F.F.C., S.K.T., H.H., M.H., A.E.H., S.C.K. and C.C.S. analyzed data; M.L. and E.S. designed and supervised the project and edited the manuscript. All authors contributed to and approved the final version of the manuscript.

**Data Availability Statement:** Data will be shared via dbGaP: https://www.ncbi.nlm.nih.gov/projects/gap/cgi-bin/study.cgi?study_id=phs002504.v1.p1.

**Conflict of Interest/Disclosures:** The authors declare no conflict of interest.

## Abstract

Mutations in five canonical Ras pathway genes (*NF1*, *NRAS*, *KRAS*, *PTPN11* and *CBL*) are detected in nearly 90% of patients with juvenile myelomonocytic leukemia (JMML), a frequently fatal malignant neoplasm of early childhood. In this report, we describe seven patients diagnosed with *SH2B3*-mutated JMML, including five patients who were found to have initiating, loss of function mutations in the gene. *SH2B3* encodes the adaptor protein LNK, a negative regulator of normal hematopoiesis upstream of the Ras pathway. These mutations were identified to be germline, somatic or a combination of both. Loss of function of LNK, which has been observed in other myeloid malignancies, results in abnormal proliferation of hematopoietic cells due to cytokine hypersensitivity and activation of the JAK/STAT signaling pathway. *In vitro* studies of induced pluripotent stem cell-derived JMML-like hematopoietic progenitor cells (HPCs) also demonstrated sensitivity of *SH2B3*-mutated HPCs to JAK inhibition. Lastly, we describe two patients with JMML and *SH2B3* mutations who were treated with the JAK1/2 inhibitor ruxolitinib. This report expands the spectrum of initiating mutations in JMML and raises the possibility of targeting the JAK/STAT pathway in patients with *SH2B3* mutations.

## Introduction

Juvenile myelomonocytic leukemia (JMML) is a rare and aggressive overlapping myelodysplastic/myeloproliferative disorder in toddlers with a median age at onset of approximately two years[1]. Outcomes range from spontaneous remission in some patients to aggressive disease and transformation to acute myeloid leukemia in others. Most patients undergo hematopoietic cell transplantation (HCT) for curative

intent. At diagnosis, a high white blood cell (WBC) count with circulating immature myeloid cells, a peripheral monocytosis, nucleated red blood cells, thrombocytopenia, elevated fetal hemoglobin, and splenomegaly are typically observed. Fevers, cough, bloody stools, and failure to thrive may also be present. Bone marrow aspirates must display fewer than 20% blasts and can have varying degrees of abnormal erythro-, myelo- and megakaryopoiesis. Historically, laboratory features including hypersensitivity of myeloid progenitor cells to granulocyte-macrophage colony stimulating factor (GM-CSF) in colony forming assays or hyperphosphorylation of STAT5 of CD38 positive cells were used to establish a diagnosis of JMML[2]. Currently, next generation sequencing (NGS) is considered standard-of-care and allows for an accurate diagnosis as nearly all patients with JMML (~95%) have mutations detected in the Ras/MAPK signaling pathway including *CBL*, *KRAS, NF1*, *NRAS*, *RRAS, RRAS2*, and *PTPN11*[3–6]. The vast majority of these driver mutations are mutually exclusive and can be acquired in a germline and/or somatic configuration. One consequence of these mutations is hyperactivation of the Ras/MAPK pathway, including Raf/MEK/ERK. Secondary mutations at a lower allele frequency are often found outside the canonical Ras pathway and include alterations in transcription factors, epigenetic regulating genes, and the spliceosome complex. These additional mutations contribute to disease progression and predict poor outcome[3,5]. In addition to the commonly mutated genes above, oncogenic fusion proteins that lead to hyperactive Ras signaling[7–10], as well as mutations in other genes encoding for proteins upstream of the Ras pathway (e.g. *FLT3*) have been described in rare patients[10,11]. One of these upstream proteins is the lymphocyte adaptor protein LNK that is encoded by the *SH2B3* gene on chromosome 12q24.12. We previously identified seven patients with secondary

mutations in *SH2B3* in a genomic characterization of 100 patients with JMML[3]. Herein, we report seven new patients, including five with initial mutations in *SH2B3* and two with secondary *SH2B3* mutations. We also show that *SH2B3*-mutated induced pluripotent stem cell (iPSC)-derived JMML like hematopoietic progenitor cells (HPC) are sensitive to JAK inhibitors including ruxolitinib or momelotinib. Importantly, we describe two patients with *SH2B3*-mutated JMML treated with ruxolitinib who experienced clinical responses, highlighting the potential relevance of this precision medicine approach in JMML.

## Methods

*Primary patient samples*

The patients' guardians provided informed consent to this study which was reviewed and approved by the institutional review board of University of California San Francisco (IRB Number: 10-0421) in accordance with the Declaration of Helsinki. Genomic DNA from peripheral blood, bone marrow or buccal swabs was extracted using standard protocols. DNA samples were sequenced using a custom amplicon-based targeted sequencing approach. Methylation profiles were analyzed according to previously published protocols[12] and annotated according to the international, consensus definition[13]. Additional details are also described in the supplemental methods.

*Generation of iPSC*

Primary JMML and control samples were obtained at the Benioff Children's Hospital at the University of California, San Francisco or received from other pediatric

institutions via a locally-approved institutional review board research protocol. Ficoll-purified mononuclear cells from bone marrow were reprogrammed by using the Sendai virus expressing doxycycline-regulated OCT4, KLF4, MYC, and SOX2 as previously described at the Children's Hospital of Philadelphia[14]. All iPSCs studied fulfilled standard pluripotency criteria, including expression of endogenous pluripotency markers, silencing of Sendai virally-encoded reprogramming genes, and formation of all three germ-cell layers. A list of iPSCs generated for this study can be found in the supplemental material (Supplemental Table 1).

*Differentiation of iPSC to HPC*

Control and JMML iPSCs were differentiated by culturing cells in serum-free media with sequential combinations of cytokines (all growth factor reagents from R&D Systems) to support multipotent hematopoietic progenitor formation as previously described[15]. Additional details are also described in the supplemental methods.

*Cell viability assay*

The half-maximal inhibitory concentration ($IC_{50}$) for each kinase inhibitor was determined by performing luminescence-based Cell Titer Glo assays (Promega) according to the manufacturer's protocol with readout at 72 hours (h). Each agent (ruxolitinib, momelotinib, tofacitinib) was tested at three different times with each concentration tested in triplicate.

*iPSC-derived HPC drug discovery screen*

A small molecule discovery screen was performed in collaboration with the UCSF Small Molecule Discovery Center in HPCs collected on day 10 of monolayer

differentiation from iPSCs carrying the aforementioned mutations. Five thousand HPCs were plated into each well of a 384-well assay plate in 50 µl of HPC-propagating media and treated with the compound library of approximately 2000 bioactive substances at 125 nM for 72h in triplicates. The effect on viability was measured using Cell Titer Glo assays as above. Percent inhibition was calculated relative to positive and negative controls with negative control equivalent to 0% inhibition (no compound added) and positive control equivalent to 100% inhibition (no cells added). Percent inhibition of each mutant line was then compared to the percent inhibition of the wild type/non-mutant (WT) control. Additionally, hits against single-mutant HPCs were compared with hits against double-mutant HPCs. Statistical analyses and graphic data display were performed with R (Version 3.6).

*Single-cell DNA and protein sample preparation, sequencing, and data analysis*

Unsorted mononuclear cells from patient UPN2861 at the time of diagnosis were analyzed using a single-cell microfluidic approach with molecular barcode technology. Details of this approach including generation of the phylogenetic tree are described in the supplemental methods (incl Supplemental Table 5).

## Results

*SH2B3 mutations frequently co-occur with PTPN11*

We identified germline and/or somatic mutations in *SH2B3* in patients that met criteria for JMML that resulted in a truncated LNK protein or affected the biologically important SH2 domain (Figure 1, Supplemental Figure 2). Molecular and clinical characteristics of the 7 patients reported for the first time are summarized in Table 1

and 2 respectively. Including previously reported cases[3], seven of 14 patients with *SH2B3*-mutated JMML also harbored somatic *PTPN11* mutations.

*iPSC-derived HPCs recapitulate JMML*

To investigate the cooperative nature of *SH2B3* and *PTPN11* mutations, we generated iPSC-derived HPCs with one or both mutations. To confirm that HPCs recapitulate JMML, we performed colony formation assays at increasing doses of GM-CSF. While WT HPCs form almost no colonies in the absence of GM-CSF, *PTPN11*-mutant and *PTPN11*/*SH2B3*-mutant HPCs formed significantly more colonies (Supplemental Figure 3A; $p = 0.0004$ for WT vs *PTPN11* and $p < 0.0001$ for WT vs *PTPN11/SH2B3*). Mutant HPCs derived from iPSCs showed spontaneous proliferation independent of GM-CSF, an important hallmark of JMML. Elevated signaling of STAT5 and ERK, another characteristic of JMML cells, was also observed in HPCs, more prominent in the *PTPN11/SH2B3* double-mutant HPCs (Supplemental Figure 3B).

*Drug discovery screen identifies JAK inhibitor to have a differential effect on cell proliferation depending on mutational background*

In an independent high-throughput drug discovery screen performed using single- and double-mutant iPSC-derived JMML-like HPCs, we identified multiple JAK1/2 inhibitors amongst the top 10 compounds that showed a greater inhibition of *PTPN11/SH2B3*-mutant HPCs compared to *PTPN11*-mutant HPCs (Figure 2A, Supplemental Table 2).

*SH2B3-mutant HPCs are more sensitive to JAK inhibitor therapy*

To validate the drug discovery screen, we analyzed cell proliferation of iPSC-derived HPCs with different mutational backgrounds after exposure to various JAK inhibitors, including ruxolitinib, momelotinib, and tofacitinib. Hematopoietic progenitor cells with alterations in *SH2B3* were more sensitive to chemical JAK inhibition compared to HPCs not harboring mutations in *SH2B3*. This finding was observed for all JAK inhibitors but was most striking for ruxolitinib (Figure 2B).

*Single cell sequencing reveals the phylogenetic origin in a patient with concomitant SH2B3 and PTPN11 mutations*

We identified a patient with a *PTPN11* p.A72T mutation at an unusually high VAF (83%) along with a *SH2B3* p.M268I mutation (VAF 86%). This previously healthy 4-year-old male (UPN2861) was diagnosed with JMML after clinical presentation with petechiae and splenomegaly and a CBC with leukocytosis (WBC 501,000/µL), severe thrombocytopenia (platelet count 13,000/µL), and monocytosis (absolute monocyte count >8000). Fetal hemoglobin was elevated at 65% and cytogenetic and FISH analyses were normal. To determine the sequence of mutational acquisition, single-cell sequencing was performed, which revealed that a somatic *SH2B3* p.M268I was the initial mutation, which then branched into a *PTPN11* p.A72T population and a homozygous *SH2B3* p.M268I population (Figure 3, Supplemental Table 3).

*Homozygous or heterozygous SH2B3 mutations in the germline can lead to JMML*

Recognizing that mutations in *SH2B3* can initiate JMML, we screened additional JMML patients without any known driver mutation. A male (UPN3426) with consanguineous parents was born at 33 weeks gestational age via cesarean section for intrauterine growth retardation and was found to have intracranial and intrahepatic calcifications, hepatosplenomegaly, and thrombocytopenia as well as leukocytosis with monocytosis. An extensive infectious disease workup was negative. Bone marrow examination (Supplemental Figure 1C-D) revealed 9% myeloblasts and cytogenetic analysis demonstrated a normal male karyotype and a diagnosis of JMML was established. The patient developed progressive splenomegaly, portal hypertension and transfusion dependency and was started on low-dose cytarabine and 6-mercaptopurine. Symptoms improved and both medications were eventually discontinued by 20 months of life. The patient has since developed thrombocytosis (platelets 800 - 1200 $x10^9$ per liter) and continues to have splenomegaly but is otherwise asymptomatic and thriving. NGS identified a germline *SH2B3* p.L438R mutation (VAF 100%) in the patient and both parents were found to be heterozygous germline carriers of the same mutation.

A female (UPN3436) with consanguineous parents was born at term via cesarean section and was found to have low birth weight and hepatosplenomegaly. She was admitted for neonatal jaundice. At the age of 4 months, she presented with recurrent fever and diarrhea. A complete blood count demonstrated leukocytosis, anemia and thrombocytopenia. An extensive infectious and metabolic disease workup was negative. Bone marrow examination revealed dysmegakaryopoiesis with 4% blasts

(Supplemental Figure 1E-F). A diagnosis of JMML was established and the patient underwent HCT. NGS of the peripheral blood sample revealed a *SH2B3* p.R392Q mutation (VAF 100%). Sanger sequencing of a buccal swab demonstrated the same homozygous *SH2B3* mutation. Parental DNA was not available for testing.

A 2-month-old female (UPN1744) presented with leukocytosis, thrombocytopenia and splenomegaly. A peripheral blood smear demonstrated circulating myeloid precursor cells and a bone marrow aspirate was consistent with JMML. She was briefly treated with low-dose cytarabine before receiving a 4/6 human leukocyte antigen-matched unrelated cord blood transplant after conditioning with busulfan, cyclophosphamide, melphalan and anti-thymocyte globulin. The patient developed chronic GvHD of the skin but is currently alive and well with no signs of disease 14 years post-transplant. NGS of the peripheral blood identified a *SH2B3* p.Q251* mutation (VAF 63%). Sanger sequencing of T cells confirmed the same heterozygous mutation in the germline. Parental DNA was not available for testing.

*Ruxolitinib led to resolution of splenomegaly in a patient with secondary SH2B3 mutations*

A previously healthy, 5-year-old female (UPN3037) presented with fever, leukocytosis, monocytosis, thrombocytopenia and splenomegaly. Fetal hemoglobin was elevated at 63.3% and bone marrow examination showed 6% atypical myeloid blasts. Cytogenetic and FISH analysis were normal. DNA sequencing detected a primary mutation in *PTPN11* p.E76V (46% VAF) and two secondary *SH2B3* mutations including p.Q408fs (38% VAF) and p.E523fs (18% VAF). The diagnosis of

JMML was established and the patient was started on ruxolitinib at 50mg/$m^2$ by mouth twice a day. Ten days into ruxolitinib monotherapy, the patient's WBC and monocytosis decreased and abdominal ultrasound showed resolution of splenomegaly. Bone marrow examination following 10 days of ruxolitinib monotherapy revealed the VAF of the *SH2B3* mutation at p.Q408fs decreased to 22%, while the *SH2B3* mutation at p.E523fs was no longer detectable. However, the *PTPN11* p.E76V mutation was unchanged, and a new *NRAS* p.G12D mutation was detected at 4% VAF (Figure 4). Fludarabine 30mg/$m^2$ daily for 5 days and cytarabine 2g/$m^2$ daily for 5 days were added to ruxolitinib, but the patient experienced progressive disease. The patient was then treated sequentially with trametinib and azacitidine but progressed after each treatment. The patient received a haploidentical HCT from her mother following a conditioning regimen with busulfan, cyclophosphamide, thiotepa, anti-thymocyte globulin and total body irradiation. The patient relapsed by day +90 and subsequently received a paternal haploidentical HCT. The patient developed idiopathic pulmonary syndrome and died of respiratory failure in a molecular remission from JMML at day +60.

*Ruxolitinib as a bridge to HCT in a patient with SH2B3-mutated JMML*

A 4-month-old male (UPN3160) was diagnosed with JMML after presenting with anemia, leukocytosis with peripheral monocytosis, 5% circulating myeloblasts, and hepatosplenomegaly. A bone marrow biopsy revealed myeloid hyperplasia (Supplemental Figure 1A) and cytogenetic and FISH analysis were normal. DNA sequencing revealed a *SH2B3* p. M211fs*57 mutation at 50% VAF in the germline and 100% VAF in the tumor due to copy neutral loss of heterozygosity from 12q21.1

to 12q24.33. The germline mutation was discovered to be maternally inherited. A diagnosis of JMML was made and the patient was started on 6-mercaptopurine, but splenomegaly persisted. The patient was then started on ruxolitinib monotherapy at 15 mg/m$^2$ by mouth twice daily which led to complete resolution of splenomegaly, but no change in the VAF of the *SH2B3* mutation which remained at 100%. The patient was bridged to HCT with single agent ruxolitinib and is now in a molecular remission two years post-transplant.

## Discussion

LNK is a member of the SH2-B family of adaptor proteins that share three functional domains: a dimerization domain at the N terminus, a central pleckstrin homology (PH) domain and a C-terminal Src homology 2 (SH2) domain. LNK is mainly expressed in hematopoietic cells, particularly in hematopoietic stem cells[16]. Most of the protein remains in the cytoplasm, specifically, the perinuclear region[17,18]. However, the PH domain allows for binding to the plasma membrane via interaction with membrane phospholipids. The SH2 domain is responsible for most of the biological effect of LNK through interaction with phosphorylated signaling partners including cytokine and tyrosine kinase receptors (e.g. EPO, TPO, SCF) and kinases (e.g. JAK2)[19,20].

The generation of LNK-deficient mice elucidated the role of LNK in hematopoiesis: *Lnk*$^{-/-}$ mice developed features of myeloproliferative disease including splenomegaly, increased numbers of myeloid progenitors and extramedullary hematopoiesis[16,21]. A significant accumulation of pro- and pre-B cells were also noted in *Lnk*$^{-/-}$ mice demonstrating a role of LNK as negative regulator in B-lymphopoiesis[22]. These

observations are thought to be caused (at least in part) by the hypersensitivity of *Lnk*$^{-/-}$ progenitors to several cytokines with increased activation of STAT3, STAT5, AKT and MAPK signaling pathway[23].

It is therefore not surprising that mutations in *SH2B3* have been identified in a variety of hematological malignancies[24]. Mutations in *SH2B3* have been reported in 5-7% of patients with myeloproliferative neoplasms (MPNs) across all subtypes[25–27] and increase up to 13% upon leukemic transformation[28]. *SH2B3* mutations have also been described in lymphoid malignancies albeit at a much lower frequency[27,29]. In a previous study of 100 patients with JMML, we identified the first seven patients with *SH2B3* mutations[3]. While six of the previously reported patients harbored secondary *SH2B3* mutations in addition to known JMML driver mutations like *NF1* or *PTPN11*, one patient had a germline heterozygous *SH2B3* mutation without additional somatic mutations (Supplemental Table 4). Here, we present five patients with initial mutations and two patients with secondary mutations in *SH2B3* (Table 1). Due to the absence of other disease driving alterations in patients UPN3426, UPN3436, and UPN3160 as well as a lower allele frequency for the *NF1* mutation in UPN1744 (Table 1), we presume that *SH2B3* mutations initiated JMML in these four patients. Phylogenetic analysis of UPN2861's sample using single-cell DNA sequencing determined that the initiating mutation was in *SH2B3*, which then branched into discrete subclones, one of which acquired a secondary *PTPN11* mutation. Methylation profiling showed a low methylation signature for patients UPN3426, UPN3436, and UPN3160 harboring a germline *SH2B3* mutation. Patients UPN2861, UPN3037 and UPN2823 who had multiple mutations present at diagnosis, were categorized as having high methylation signatures. These data are consistent with

previous reports that altered methylation frequently accompanies the presence of secondary mutations[5,13,30].

Several groups have functionally validated *SH2B3* mutations and demonstrated that point mutations in the PH domain impair translocation to the plasma membrane and thus reduce its regulatory function[18], while mutations in the SH2 domain affect interaction with JAK/STAT and result in a more severe phenotype[19,20]. The mutations identified here result in a truncated protein (patients UPN 3160, UPN2823 and UPN1744) or affect the biologically important SH2 domain (patient UPN3426; Figure 1). Interestingly, copy-neutral loss of heterozygosity of *SH2B3* in patient UPN3160 associated with uniparental isodisomy is a mechanism that has been observed commonly in other cancers and specifically in JMML with *CBL* and *NF1* [31,32].

In general, there is remarkable similarity between *SH2B3*-mutated JMML and *CBL*-mutated JMML. Both are associated with germline mutations (including heterozygous germline mutations without any somatic events), can occur in the context of a constitutional syndrome, can lead to upregulation of the JAK-STAT pathway, can be associated with copy neutral LOH in the tumor, and is often manifested by a spontaneously remitting form of JMML. *SH2B3*-mutated JMML also shares similarities with myeloproliferative disorders (MPD) seen in infants with Noonan syndrome, most commonly caused by germline mutations in *PTPN11*. Both can present in the context of a constitutional syndrome and can manifest with a transient MPD of infancy. Although limited by very small numbers, the severity of the myeloproliferation in our cohort appeared to differ based on whether the *SH2B3* mutations were germline or somatic and whether the former were monoallelic or biallelic. In general, germline mutations were associated with less aggressive disease compared to somatic mutations. Larger studies will be required to validate

these initial findings and to determine their exact classification as an MPD, MPN/MDS or JMML.

A schematic overview of all *SH2B3* mutations identified in JMML to this date is highlighted in Figure 1. We observed a striking association between *SH2B3* and *PTPN11* with seven of 14 patients harboring both mutations (Supplemental Figure 4). Of note, *SH2B3* and *PTPN11* are located in close proximity at 12q24.12 and 12q24.13, respectively. We observed copy neutral loss of heterozygosity causing elevated VAFs in *SH2B3* and *PTPN11* above what is typically observed in cases with *PTPN11* mutations alone. To model the cooperative nature of these mutations, we engineered iPSC-derived HPCs with one or both mutations and observed increased pSTAT5 and pERK signaling in the cells with both mutations compared to one alone. Since *in vitro* data showed that loss of LNK results in increased JAK/STAT signaling, we hypothesize that this cohort of patients may benefit from JAK inhibitor therapy. Our data from iPSC-derived JMML-like HPCs shows that those cells with secondary *SH2B3* mutations are more sensitive to JAK inhibitors, including ruxolitinib and momelotinib, that are FDA/EMA-approved or under clinical investigation in adults with MPNs.[33–35] It is important to note that our iPSC data highlights the efficacy of ruxolitinib in *SH2B3*-mutated JMML but cannot provide insight into the potential relevance of the sequence to acquisition of each mutation. Our findings are consistent with a previous study in iPSCs that also demonstrated that JAK inhibitor therapy could be beneficial in *CBL*-mutated JMML[36]. Following a 10-day treatment with ruxolitinib, patient UPN3037, who harbored a *PTPN11* and two *SH2B3* alterations at diagnosis, demonstrated decreased WBC and improved splenomegaly. Importantly, the *SH2B3* p.E523fs mutation was no longer detectable and the *SH2B3* p.Q408fs allele frequency reduced from 38% to 11% (Figure 4) while

receiving ruxolitinib monotherapy. However, ruxolitinib did not have any appreciable effect on the initiating *PTPN11* mutation and the patient experienced progressive disease. Additionally, patient UPN3160 experienced a rapid resolution of splenomegaly after one cycle of ruxolitinib monotherapy and served as a bridge to HCT.

We have previously reported on a JMML patient with a heterozygous germline *SH2B3* mutation[3]. Here, we have shown that heterozygous germline *SH2B3* mutations can become homozygous in hematopoietic cells due to copy neutral loss of heterozygosity and that homozygous germline *SH2B3* mutations can all converge on causing JMML. Lastly, we identified a patient with *PTPN11 and SH2B3*-mutated JMML, who using single cell sequencing, we have now shown had an initiating somatic mutation in *SH2B3*.

In summary, this report expands the spectrum of driver mutations in JMML that lead to MAPK activation to include *SH2B3,* and highlights JAK/STAT inhibition as a possible targeted treatment for these patients.

**List of Abbreviations:**

| | |
|---|---|
| AOC | Antibody-oligo conjugate |
| DAb-seq | DNA plus antibody sequencing |
| GM-CSF | Granulocyte-macrophage colony stimulating factor |
| GvHD | Graft-versus-host disease |
| HCT | Hematopoietic cell transplantation |
| HPC | Hematopoietic progenitor cell |
| iPSC | Induced pluripotent stem cell |
| JMML | Juvenile myelomonocytic leukemia |
| MPD | Myeloproliferative disorder |
| MPN | Myeloproliferative neoplasm |
| NGS | Next-generation sequencing |
| PH | Pleckstrin homology |
| SC DNA | Single cell DNA |
| SH2 | Src homology 2 |
| WBC | White blood count |
| WT | Wild type |

## References


1. Locatelli F, Niemeyer CM. How I treat juvenile myelomonocytic leukemia. Blood. 2018;125(7):1083-1091.
2. Emanuel PD, Bates LJ, Castleberry RP, Gualtieri RJ, Zuckerman KS. Selective hypersensitivity to granulocyte-macrophage colony-stimulating factor by juvenile chronic myeloid leukemia hematopoietic progenitors. Blood. 1991;77(5):925-929.
3. Stieglitz E, Taylor-Weiner AN, Chang TY, et al. The Genomic Landscape of Juvenile Myelomonocytic Leukemia. Nat Genet. 2015;47(11):1326-1333.
4. Caye A, Strullu M, Guidez F, et al. Juvenile myelomonocytic leukemia displays mutations in components of the RAS pathway and the PRC2 network. Nat Genet. 2015;47(11):1334-1340.
5. Murakami N, Okuno Y, Yoshida K, et al. Integrated molecular profiling of juvenile myelomonocytic leukemia. Blood. 2018;131(14):1576-1586.
6. Wintering A, Dvorak CC, Stieglitz E, Loh ML. Juvenile myelomonocytic leukemia in the molecular era: a clinician's guide to diagnosis, risk-stratification, and treatment. Blood Adv. 2021;5(22):4783-4793.
7. Buijs A, Bruin M. Fusion of FIP1L1 and RARA as a result of a novel t(4;17)(q12;q21) in a case of juvenile myelomonocytic leukemia. Leukemia. 2007;21(5):1104-1108.
8. Morerio C, Acquila M, Rosanda C, et al. HCMOGT-1 is a novel fusion partner to PDGFRB in juvenile myelomonocytic leukemia with t(5;17)(q33;p11.2). Cancer Res. 2004;64(8):2649-2651.
9. Byrgazov K, Kastner R, Dworzak M, et al. A Novel Fusion Gene NDEL1-Pdgfrb in a Patient with JMML with a New Variant of TKI-Resistant Mutation in the Kinase Domain of PDGFRβ. Blood. 2014;124(21):613.
10. Chao AK, Meyer JA, Lee AG, et al. Fusion driven JMML: a novel CCDC88C–FLT3 fusion responsive to sorafenib identified by RNA sequencing. Leukemia. 2020;34(2):662-666.
11. Gratias EJ, Liu YL, Meleth S, Castleberry RP, Emanuel PD. Activating FLT3 mutations are rare in children with juvenile myelomonocytic leukemia. Pediatr Blood Cancer. 2005;44(2):142-146.
12. Behnert A, Meyer J, Parsa J-Y, et al. Exploring the Genetic and Epigenetic Origins of Juvenile Myelomonocytic Leukemia using Newborn Screening Samples. Leukemia. 2022;36(1):279-282.
13. Schönung M, Meyer J, Nöllke P, et al. International Consensus Definition of DNA Methylation Subgroups in Juvenile Myelomonocytic Leukemia. Clin Cancer Res. 2020;27(1):158-168.
14. Gandre-Babbe S, Paluru P, Aribeana C, et al. Patient-derived induced pluripotent stem cells recapitulate hematopoietic abnormalities of juvenile myelomonocytic leukemia. Blood. 2013;121(24):4925-4929.

15. Mills JA, Paluru P, Weiss MJ, Gadue P, French DL. Hematopoietic differentiation of pluripotent stem cells in culture. Methods Mol Biol. 2014;1185:181-194.

16. Velazquez L, Cheng AM, Fleming HE, et al. Cytokine signaling and hematopoietic homeostasis are disrupted in Lnk-deficient mice. J Exp Med. 2002;195(12):1599-1611.

17. Li Y, He X, Schembri-King J, Jakes S, Hayashi J. Cloning and characterization of human Lnk, an adaptor protein with pleckstrin homology and Src homology 2 domains that can inhibit T cell activation. J Immunol. 2000;164(10):5199-5206.

18. Gery S, Gueller S, Chumakova K, Kawamata N, Liu L, Koeffler HP. Adaptor protein Lnk negatively regulates the mutant MPL, MPLW515L associated with myeloproliferative disorders. Blood. 2007;110(9):3360-3364.

19. Tong W, Zhang J, Lodish HF. Lnk inhibits erythropoiesis and Epo-dependent JAK2 activation and downstream signaling pathways. Blood. 2005;105(12):4604-4612.

20. Bersenev A, Wu C, Balcerek J, Tong W. Lnk controls mouse hematopoietic stem cell self-renewal and quiescence through direct interactions with JAK2. J Clin Invest. 2008;118(8):2832-2844.

21. Takaki S, Morita H, Tezuka Y, Takatsu K. Enhanced hematopoiesis by hematopoietic progenitor cells lacking intracellular adaptor protein, Lnk. J Exp Med. 2002;195(2):151-160.

22. Takaki S, Sauer K, Iritani BM, et al. Control of B cell production by the adaptor protein lnk. Definition Of a conserved family of signal-modulating proteins. Immunity. 2000;13(5):599-609.

23. Takizawa H, Eto K, Yoshikawa A, Nakauchi H, Takatsu K, Takaki S. Growth and maturation of megakaryocytes is regulated by Lnk/Sh2b3 adaptor protein through crosstalk between cytokine- and integrin-mediated signals. Exp Hematol. 2008;36(7):897-906.

24. Maslah N, Cassinat B, Verger E, Kiladjian JJ, Velazquez L. The role of LNK/SH2B3 genetic alterations in myeloproliferative neoplasms and other hematological disorders. Leukemia. 2017;31(8):1661-1670.

25. Mcmullin MF, Cario H. LNK mutations and myeloproliferative disorders. Am J Hematol. 2016;91(2):248-251.

26. Gundabolu K, Dave BJ, Alvares CJ, et al. The Missing LNK□: Evolution from Cytosis to Chronic Myelomonocytic Leukemia in a Patient with Multiple Sclerosis and Germline SH2B3 Mutation. Case Rep Genet. 2022:2022:6977041.

27. Perez-Garcia A, Ambesi-Impiombato A, Hadler M, et al. Genetic loss of SH2B3 in acute lymphoblastic leukemia. Blood. 2013;122(14):2425-2432.

28. Pardanani A, Lasho T, Finke C, Oh ST, Gotlib J, Tefferi A. LNK mutation studies in blast-phase myeloproliferative neoplasms, and in chronic-phase disease with TET2, IDH, JAK2 or MPL mutations. Leukemia.

2010;24(10):1713-1718.

29. Zhang J, Ding L, Holmfeldt L, et al. The genetic basis of early T-cell precursor acute lymphoblastic leukaemia. Nature. 2012;481(7380):157-163.

30. Stieglitz E, Mazor T, Olshen AB, et al. Genome-wide DNA methylation is predictive of outcome in juvenile myelomonocytic leukemia. Nat Commun. 2017;8(1):1-8.

31. Stephens K, Weaver M, Leppig KA, et al. Interstitial uniparental isodisomy at clustered breakpoint intervals is a frequent mechanism of NF1 inactivation in myeloid malignancies. Blood. 2006;108(5):1684-1689.

32. Le DT, Kong N, Zhu Y, et al. Somatic inactivation of Nf1 in hematopoietic cells results in a progressive myeloproliferative disorder. Blood. 2004;103(11):4243-4250.

33. Xu L, Feng J, Gao G, Tang H. Momelotinib for the treatment of myelofibrosis. Expert Opin Pharmacother. 2019;20(16):1943-1951.

34. Griesshammer M, Sadjadian P. The BCR-ABL1-negative myeloproliferative neoplasms: a review of JAK inhibitors in the therapeutic armamentarium. Expert Opin Pharmacother. 2017;18(18):1929-1938.

35. Pardanani A, Vannucchi AM, Passamonti F, Cervantes F, Barbui T, Tefferi A. JAK inhibitor therapy for myelofibrosis: critical assessment of value and limitations. Leukemia. 2011;25(2):218-225.

36. Tasian SK, Casas JA, Posocco D, et al. Mutation-Specific Signaling Profiles and Kinase Inhibitor Sensitivities of Juvenile Myelomonocytic Leukemia Revealed by Induced Pluripotent Stem Cells. Leukemia. 2018;33(1):181-190.

37. Jahn K, Kuipers J, Beerenwinkel N. Tree inference for single-cell data. Genome Biol. 2016;17:86.

## Tables

**Table 1.** Molecular characteristics of the 7 patients with *SH2B3* mutations.

| UPN | Sex | Age at diagnosis | *SH2B3* - *primary or secondary* | *SH2B3* alteration (VAF%) | Configuration of *SH2B3* alteration | Other additional alterations (VAF%) | Cytogenetic abnormalities | Methylation profile |
|---|---|---|---|---|---|---|---|---|
| UPN2861 | M | 4y | Primary | p.M268I (86%) | Somatic | *PTPN11* p.A72T (83%); *WT1* p.K492Q (12%); *IKZF1* p.F154Y (8%) | No | High |
| UPN3426 | M | 0m | Primary | p.L438R (100%) | Germline | None | No | Low |
| UPN3436 | F | 4m | Primary | p.R392Q (100%) | Germline | None | No | Not available |
| UPN1744 | F | 2m | Primary | p.Q251* (63%) | Germline | *NF1 p.Y628fs (5%)* | No | Low |
| UPN3037 | F | 5.8y | Secondary | p.Q408fs (38%); p.E523fs (18%) | Somatic | *PTPN11* p.E76V (46%) | No | High |
| UPN3160 | M | 4m | Primary | p.M211fs*57 (100%) | Germline | None | No | Low |
| UPN2823 | M | 6y | Unknown | p. R308* (46%); p.G225fs*47 (21%) | Somatic | *RRAS* p.Q72L (40%); *ZRSR2* p.Q255 (19%); *PTPN11* p.T73I (4%) | No | High |

**Table 2:** Clinical characteristics of the 7 patients with *SH2B3* mutations.

| Case ID | Hb at diagnosis (g/dL) | WBC at diagnosis (n/µL) | Platelets at diagnosis (n/µL) | Monocytes at diagnosis (n/µL) | HbF at diagnosis | Peripheral blast count at diagnosis (%) | Splenomegaly at diagnosis? | Circulating myeloid or erythroid precursors? | Treatment | Ruxolitinib? | Outcome |
|---|---|---|---|---|---|---|---|---|---|---|---|
| UPN2861 | 11.1 | 501000 | 13000 | >8000 | Elevated | 6% | Yes | Yes | HCT | No | Deceased |
| UPN3426 | 11.2 | 69700 | 49000 | 3100 | Not performed | 9% | Yes | Yes | Chemotherapy | No | Alive |
| UPN3436 | 10 | 102000 | 75000 | 13000 | Elevated | 5% | Yes | Yes | HCT | No | Alive |
| UPN1744 | 9.9 | 84900 | 50000 | Unknown | Not done | Unknown | Yes | Yes | HCT | No | Alive |
| UPN3037 | 10.7 | 67000 | 102000 | 7140 | Elevated | 6% | Yes | Yes | HCT | Yes | Deceased |
| UPN3160 | 9.8 | 114000 | 181000 | 10000 | Normal | 5% | Yes | Yes | HCT | Yes | Alive |
| UPN2823 | 10.2 | 11400 | 116000 | 1630 | Elevated | 12% | Yes | Yes | HCT | No | Alive |

## Figure Legends

**Figure 1.** Schematic overview of *SH2B3* including the location of both primary and secondary mutations described in JMML. The top row shows the mutations of the 7 novel patients reported here; the bottom row shows the location of the mutations previously reported by our group[3]. Highlighted in red boxes are those mutations that are considered JMML-initiating. Alterations that co-exist with a *PTPN11* mutation are displayed with a dashed line.

**Figure 2.** *SH2B3*-mutated HPCs are more sensitive to JAK inhibitor therapy. (A) Linear regression plot of high throughput drug discovery screen comparing drug inhibition of *PTPN11/SH2B3* double-mutant HPC versus *PTPN11* single-mutant HPC: The top ten hits that inhibit growth of double-mutant HPC to a greater extent than of single-mutant HPC, include two JAK inhibitors: momelotinib and CEP-33779. (B) Cell viability assay readout after 72h following exposure to ruxolitinib or momelotinib in two different iPSC-derived HPC lines. Data for tofacitinib not shown.

**Figure 3.** Phylogenetic tree at diagnosis from patient UPN2861 inferred from single cell sequencing and single cell inference of tumor evolution (SCITE), a probabilistic model using a flexible Markov-chain Monte Carlo algorithm.[37] *SH2B3* p.M268I (heterozygous; HET) was the initiating mutation, which then branched into a *PTPN11* population and a homozygous (HOM) *SH2B3* population. The *PTPN11* population finally branched into a *WT1* and *IKZF1* clone.

**Figure 4.** Molecular response of patient UPN3037 who harbored a *PTPN11* and two *SH2B3* mutations at diagnosis. Following 10 days of ruxolitinib monotherapy, the *SH2B3* mutation at codon 523 was no longer detectable, and a reduction from 38% to 11% was observed for the *SH2B3* mutation at codon 408.

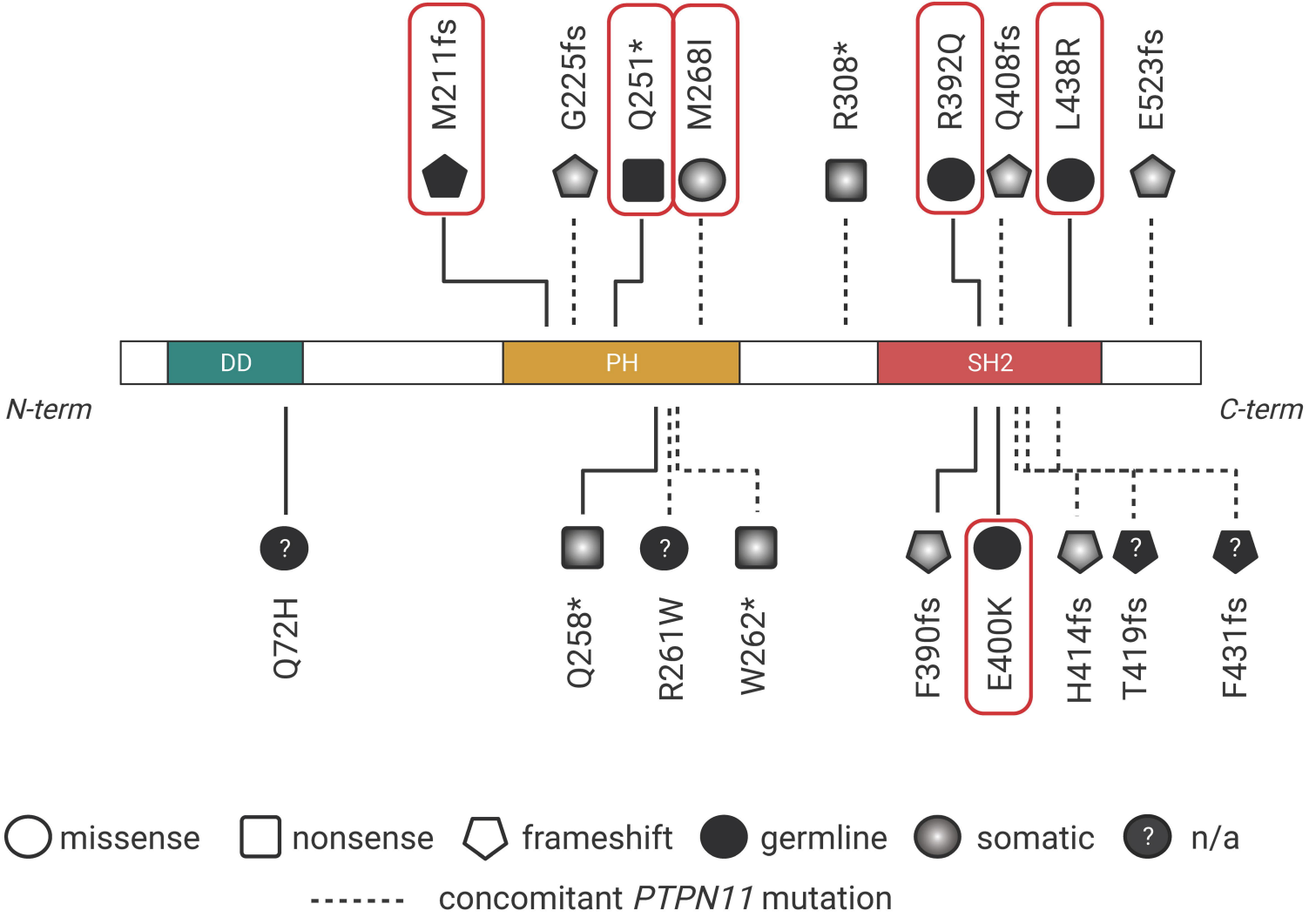
M211fs
G225fs
Q251*
M268I
R308*
R392Q
Q408fs
L438R
E523fs
DD
PH
SH2
N-term
C-term
Q72H
Q258*
R261W
W262*
F390fs
E400K
H414fs
T419fs
F431fs
missense
nonsense
frameshift
germline
somatic
n/a
concomitant PTPN11 mutation

A

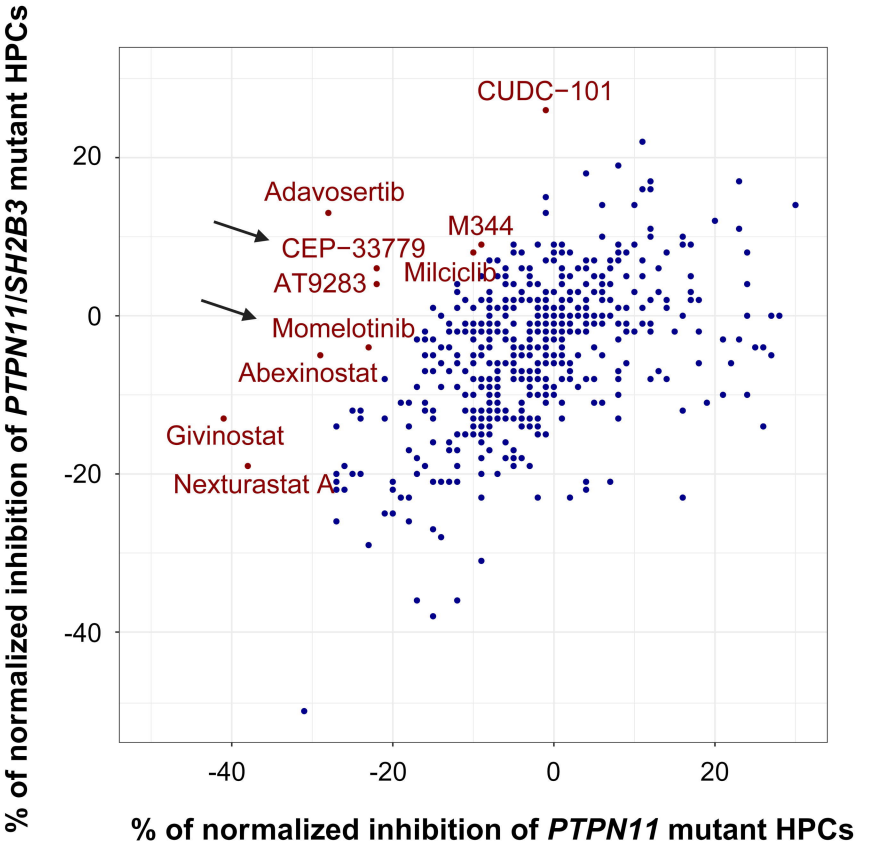
CUDC−101
Adavosertib
M344
CEP−33779
Milciclib
AT9283
Momelotinib
Abexinostat
Givinostat
Nexturastat A
20
0
-20
-40
-40
-20
0
20
% of normalized inhibition of PTPN11/SH2B3 mutant HPCs
% of normalized inhibition of PTPN11 mutant HPCs

B

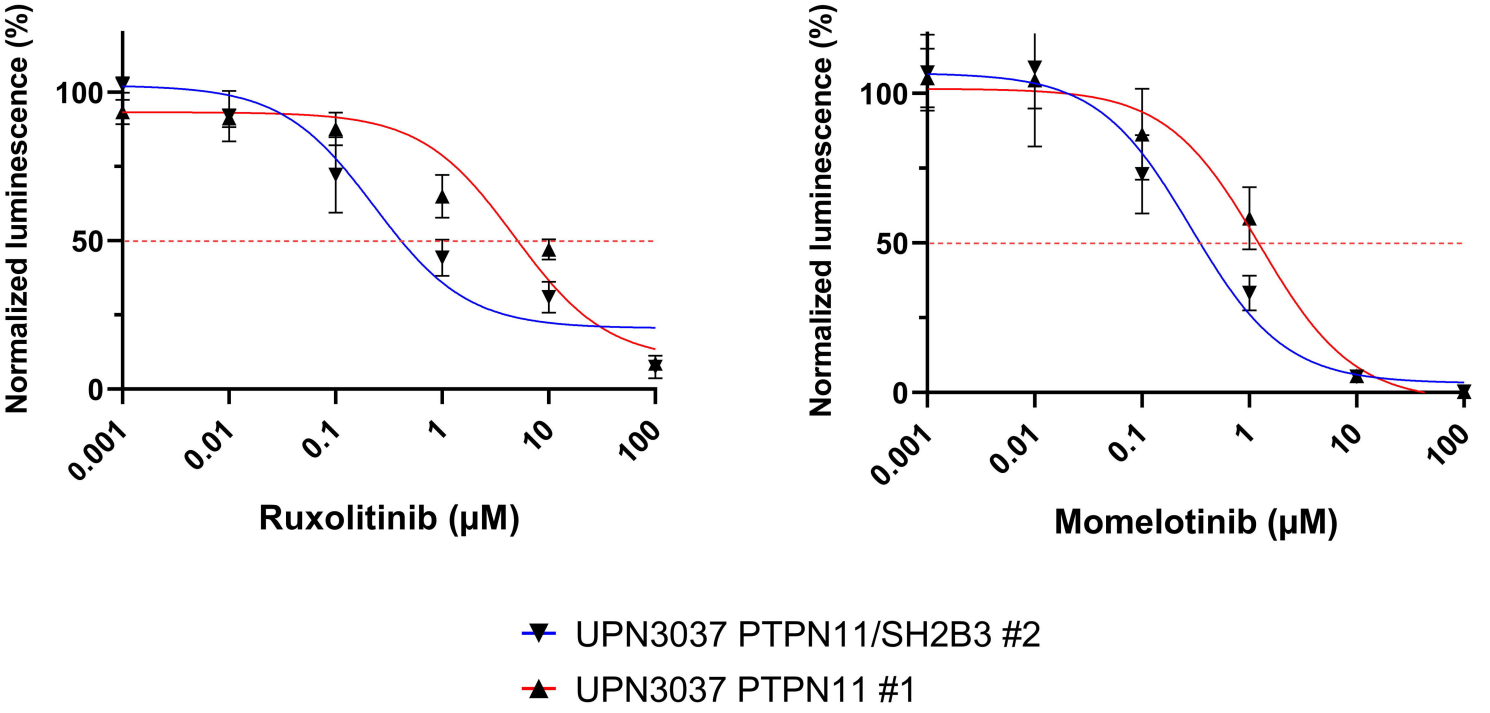
Normalized luminescence (%)
100
50
0
0.001
0.01
0.1
1
10
100
Ruxolitinib (μM)
Momelotinib (μM)
UPN3037 PTPN11/SH2B3 #2
UPN3037 PTPN11 #1

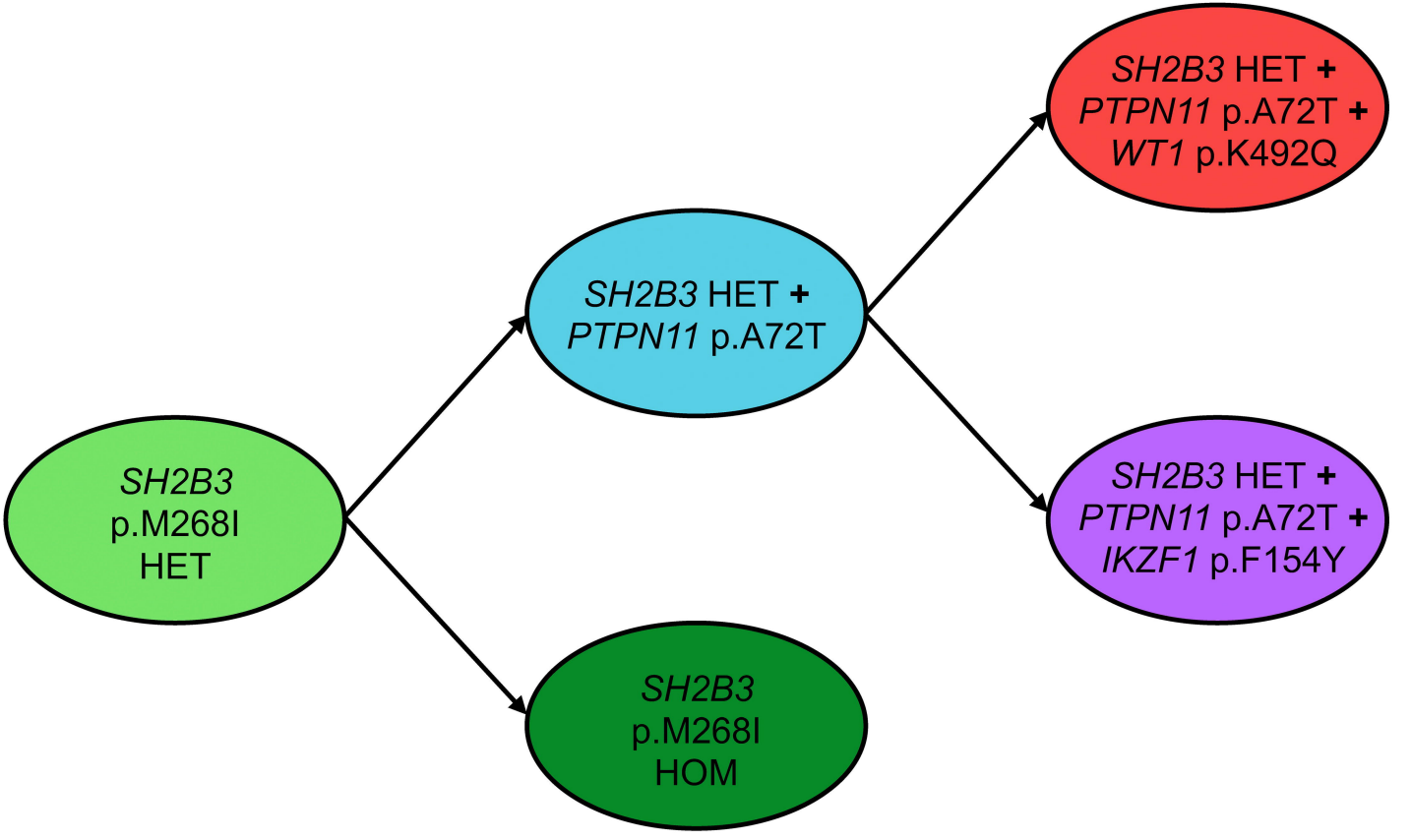
*SH2B3* p.M268I HET
*SH2B3* HET + *PTPN11* p.A72T
*SH2B3* p.M268I HOM
*SH2B3* HET + *PTPN11* p.A72T + *WT1* p.K492Q
*SH2B3* HET + *PTPN11* p.A72T + *IKZF1* p.F154Y

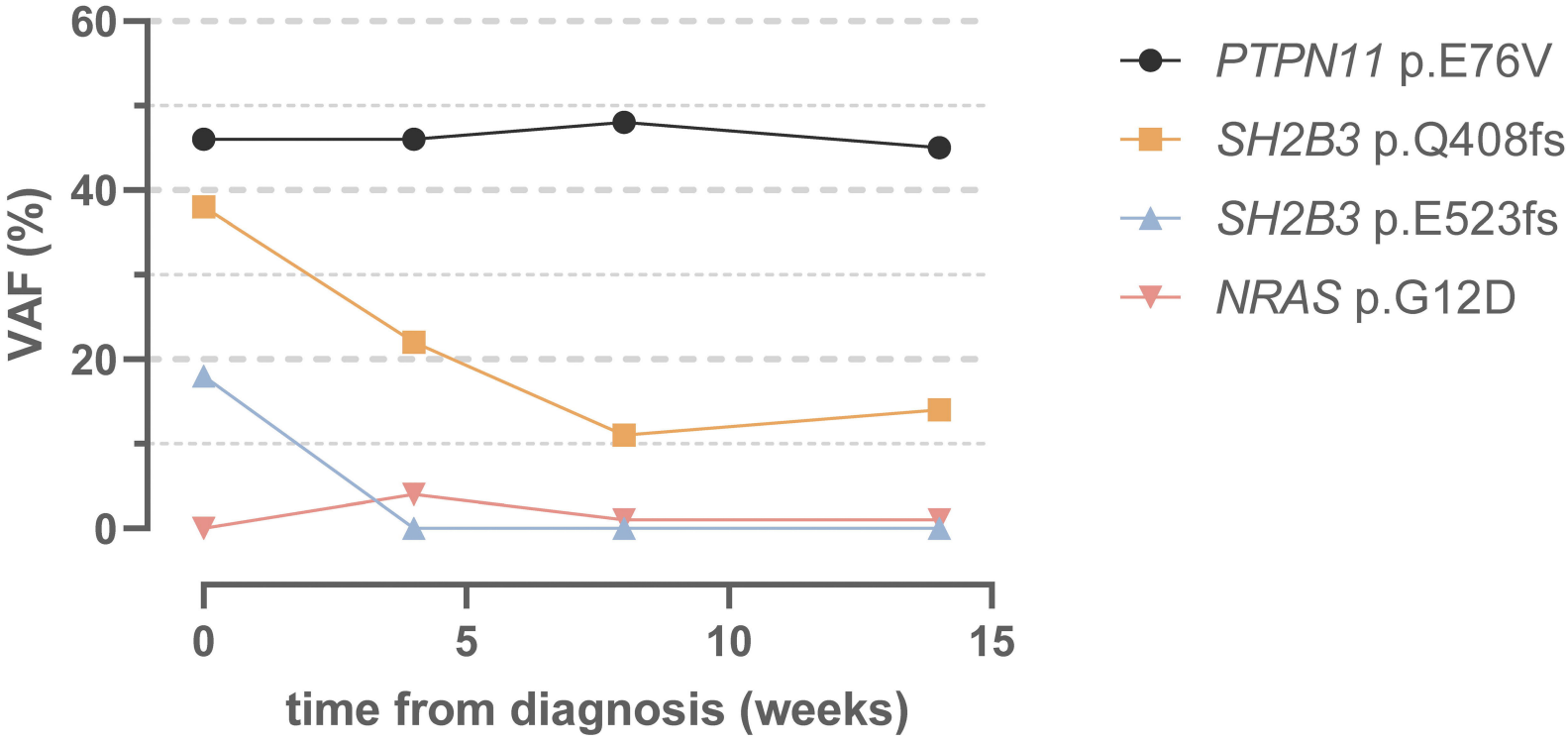
60
40
20
0
VAF (%)
0
5
10
15
time from diagnosis (weeks)
PTPN11 p.E76V
SH2B3 p.Q408fs
SH2B3 p.E523fs
NRAS p.G12D

# Supplemental Material

## Supplemental Methods

### Germline validation

To investigate the germline nature of the *SH2B3* mutation in patients UPN1744 and UPN3436 (Table 1) genomic DNA was isolated from CD3+ sorted T cells and buccal swabs, respectively. Genomic DNA was isolated and purified using the AllPrep DNA/RNA Mini kit (Qiagen) according to directions and 50-100ng of DNA used for exon specific PCR. For UPN1744, *SH2B3* exon 3 primers: F (TGGACCTCACTACAGGCTCA) and R (AATTCAGCTGCTGCTCGTCT) were used and product was Sanger sequenced. For UPN3436, *SH2B3* exon 6 primers: F (TAGCTAGGCCATTGTCTTCTGG) and R (CACGACCGAGGGAAAGTGG) were used and product was Sanger sequenced. Sanger sequences are depicted in Supplemental Figure 2.

### *Differentiation of iPSC to HPC*

Monolayer differentiation of iPSC into HPCs was started when cells were ~70% confluent and was performed as previously described[1]. In short, different base medias and cytokines (all growth factor reagents from R&D Systems) were added to promote HPC formation:

| Days | Medium | BMP-4 | VEGF | CHIR* | bFGF | SCF | Flt3L |
|---|---|---|---|---|---|---|---|
| 0-1 | RPMI | 5 | 50 | 0.5-1.0 | | | |
| 2-3 | RPMI/SP34 | 5 | 50 | | 20 | | |
| 4-5 | SP34 | | 15 | | 5 | | |
| 6 | SFD | | 50 | | 100 | 50 | 25 |
| 7-10 | SFD | | 50 | | 100 | 50 | 25 |

*CHIR concentration in µM; all other concentrations in ng/mL

All base media were supplemented with L-glutamine (2mM), penicillin/streptomycin (1x), MTG (3µL/mL of a 26µL in 2ML IMDM stock) and ascorbic acid (50µg/mL).
HPCs were than collected on day 9 or day 10 of monolayer differentiation and analyzed using flow cytometry (CD41, CD42b, CD235, CD34 and CD45; all antibodies were purchased from BioLegend).

***Single-cell DNA and Protein Sample Preparation, Library Generation, and Sequencing***

We performed single-cell DNA plus antibody sequencing (DAb-seq) on unsorted mononuclear cells using a microfluidic approach with molecular barcode technology using the Tapestri platform (MissionBio) as previously described[2,3]. Briefly, cryopreserved cells were thawed and normalized to 10,000 cells/µL in 180 µL PBS (Corning). Pooled samples were resuspended in cell buffer (MissionBio), diluted to 4-7e6 cells/mL, and then loaded onto a microfluidics cartridge, where individual cells were encapsulated, lysed, and barcoded using the Tapestri instrument. DNA from barcoded cells was amplified via PCR using a targeted panel that included 288 amplicons across 66 genes associated with acute leukemia (Supplemental Table 5). DNA PCR products were isolated, purified with AmpureXP beads (Beckman Coulter), used as a PCR template for library generation, and then repurified with AmpureXP beads. The DNA library was quantified and assessed for quality via a Qubit fluorometer (Life Technologies) and Bioanalyzer (Agilent Technologies) prior to pooling for sequencing on an Illumina Novaseq.

### *Single-Cell DAb-seq Data Processing and Analysis*

FASTQ files were processed via an open-source pipeline as described previously[2]. This analysis pipeline trims adaptor sequences, demultiplexes DNA panel amplicons and antibody tags into single cells, and aligns panel reads to the hg19 reference genome. Valid cell barcodes were called using the inflection point of the cell-rank plot in addition to the requirement that 60% of DNA intervals were covered by at least eight reads. Variants were called using GATK (v 4.1.3.0) according to GATK best practices[4]. For each valid cell barcode, variants were filtered according to quality and sequence depth reported by GATK, with low quality variants and cells excluded based on the cutoffs of quality score < 30, read depth < 10, and alternate allele frequency < 20%. We analyzed all variants present in >0.1% of cells. Variants were assessed for known or likely pathogenicity via ClinVar and COSMIC databases[5,6], and previously identified, non-intronic somatic variants were included in clonal analyses, as per prior single cell DNA (SC DNA) studies[7,8]. The patient's phylogenetic tree was inferred using single cell inference of tumor evolution (SCITE), a probabilistic model using a flexible Markov-chain Monte Carlo algorithm[9]. SCITE was employed with a global false positive rate set to 1% and a platform-provided false-negative rate, as per prior SC DNA studies[8]. Only cells with complete genotyping of variants of interest, as identified via prior bulk sequencing, were included in phylogenetic analysis.

## Supplemental Case Vignette

### *Case Vignette - UPN2823*

*A 6-year-old boy presented with 12% peripheral myeloblasts and elevated age-adjusted fetal hemoglobin. Abdominal ultrasound demonstrated splenomegaly.*

*Cytogenetic and FISH analysis were normal. DNA sequencing detected two mutations in SH2B3 p.R308* (VAF 46%) and p.G225fs*47 (VAF 21%), a mutation in RRAS2 p.Q72L (VAF 40%), a mutation in ZRSR2 p.Q255* (VAF 19%), and a PTPN11 p.T73I mutation (VAF 4%). A buccal sample was negative for all of the above mutations. Five months after diagnosis, he received allogeneic HCT from a 10/10 human leukocyte antigen-matched unrelated donor after conditioning with busulfan, cyclophosphamide, and melphalan. Following transplant, the patient developed both acute and chronic graft versus host disease (GvHD) with bronchiolitis obliterans. The patient is still receiving pulmonary therapy but does not require supplemental oxygen and currently has no signs of disease three years post-transplant.*

## Supplemental Tables

**Supplemental Table 1:** Overview of iPSC lines used in this study

| **Patient Sample ID** | **Cell Source** | **Reprogramming Vector** | **Driver Mutation** | | **Secondary Mutation** | |
|---|---|---|---|---|---|---|
| | | | **Gene** | **Mutation** | **Gene** | **Mutation** |
| **UPN3037** | BM | Sendai | *PTPN11* | +/+ | - | - |
| | | | | p.E69K/+ | - | - |
| | | | | | *SH2B3* | p.W262X<br>p.H414Y |

**Supplemental Table 2:** List of the top 10 compounds that showed a greater inhibition of *PTPN11/SH2B3* double mutant HPCs than of *PTPN11* single mutant HPCs.

| # | Drug | Target | Pathway |
|---|---|---|---|
| **1** | Adavosertib (MK-1775) | Wee1 | Cell Cycle |
| **2** | Givinostat (ITF2357) | HDAC | Cytoskeletal Signaling |
| **3** | CEP-33779 | JAK | JAK/STAT |
| **4** | CUDC-101 | EGFR, HDAC, HER2 | Epigenetics |
| **5** | AT9283 | Aurora Kinase, Bcr-Abl, JAK | JAK/STAT |
| **6** | Abexinostat (PCI-24781) | HDAC | Cytoskeletal Signaling |
| **7** | Momelotinib (CYT387) | JAK | JAK/STAT |
| **8** | Nexturastat A | HDAC | DNA Damage |
| **9** | Milciclib (PHA-848125) | CDK | Cell Cycle |
| **10** | M344 | HDAC | Cytoskeletal Signaling |

**Supplemental Table 3:** Frequencies of subclones of UPN2861 identified by single-cell sequencing.

| **Clone** | **Number of Mutated Single Cells (%)** |
|---|---|
| *SH2B3* + *PTPN11* + *IKZF1* | 20 (8.9%) |
| *SH2B3* + *PTPN11* + *WT1* | 31 (13.9%) |
| *SH2B3* + *PTPN11* | 143 (63.2%) |
| *SH2B3* | 3 (1.3%) |
| *SH2B3* - Homozygous | 4 (1.8%) |
| No detectable pathogenic mutations | 22 (9.9%) |

**Supplemental Table 4:** Previously reported patients with *SH2B3* alterations[11].

| Case ID | Sex | Age at diagnosis | *SH2B3* alteration (VAF%) | Configuration of *SH2B3* alteration | Additional alterations | Cytogenetic abnormalities | Treatment | Outcome |
|---|---|---|---|---|---|---|---|---|
| UPN1420 | M | 2y | p.F390fs (42%); p.Q258* (25%) | Somatic | *NF1* p.Y2285* (46%); *NF1* p.I679fs (38%); *ASXL1* p.Y591* (51%) | No | HCT | Deceased |
| UPN2531 | M | 3y | p.W262* (35%); p.H414fs (40%) | Somatic | *PTPN11* p.E69K (39%) | No | HCT | Deceased |
| UPN1970 | F | 7m | p.E400K (43%) | Germline | None | No | HCT | Alive |
| J295 | M | 2.5y | p.T419fs (58%) | n/a | *PTPN11* p.E76K (46%) | n/a | n/a | Deceased |
| J316 | M | 4.6y | p.F431fs (34%) | n/a | *PTPN11* p.G503A (63%); *RRAS* p.R132H (46%) | n/a | Chemotherapy | Deceased |
| J322 | M | 4.2y | p.R261W (10%) | n/a | *PTPN11* p.D61V (52%); *NF1* p.R440* (24%); *NF1* p.R1306* (13%) | n/a | HCT | Alive |
| J325 | M | 4y | p.Q72H (17%) | n/a | None | n/a | n/a | Deceased |

**Supplemental Table 5:** Amplicon panel used for single cell sequencing.

| Chromosome | Gene | Amplicon start | Amplicon end |
|---|---|---|---|
| chr1 | *PIK3CD* | 9775671 | 9775941 |
| chr1 | *PIK3CD* | 9781387 | 9781645 |
| chr1 | *PIK3CD* | 9782105 | 9782371 |
| chr1 | *PIK3CD* | 9782490 | 9782702 |
| chr1 | *PIK3CD* | 9783227 | 9783486 |
| chr1 | *PIK3CD* | 9784116 | 9784376 |
| chr1 | *PIK3CD* | 9786999 | 9787257 |
| chr1 | *CSF3R* | 36933146 | 36933346 |
| chr1 | *CSF3R* | 36933346 | 36933606 |
| chr1 | *MACF1* | 39723577 | 39723814 |
| chr1 | *NRAS* | 115256487 | 115256723 |
| chr1 | *NRAS* | 115258609 | 115258825 |
| chr1 | *RIT1* | 155880253 | 155880493 |
| chr10 | *SMC3* | 112343860 | 112344065 |
| chr10 | *SMC3* | 112356141 | 112356380 |
| chr10 | *SMC3* | 112360272 | 112360528 |
| chr10 | *SHOC2* | 112723994 | 112724234 |
| chr11 | *HRAS* | 534082 | 534333 |
| chr11 | *RRAS2* | 14316323 | 14316546 |
| chr11 | *WT1* | 32410614 | 32410840 |
| chr11 | *WT1* | 32413427 | 32413633 |
| chr11 | *WT1* | 32414189 | 32414405 |
| chr11 | *WT1* | 32439082 | 32439321 |

| | | | |
|---|---|---|---|
| chr11 | *WT1* | 32449937 | 32450197 |
| chr11 | *WT1* | 32456240 | 32456481 |
| chr11 | *KMT2A* | 118368522 | 118368745 |
| chr11 | *CBL* | 119142363 | 119142580 |
| chr11 | *CBL* | 119148869 | 119149075 |
| chr11 | *CBL* | 119149076 | 119149333 |
| chr11 | *CBL* | 119149338 | 119149575 |
| chr11 | *CBL* | 119168935 | 119169145 |
| chr11 | *CBL* | 119170258 | 119170486 |
| chr12 | *KDM5A* | 420042 | 420282 |
| chr12 | *KDM5A* | 430179 | 430396 |
| chr12 | *KDM5A* | 443425 | 443663 |
| chr12 | *ETV6* | 11992084 | 11992315 |
| chr12 | *ETV6* | 12006322 | 12006542 |
| chr12 | *ETV6* | 12022379 | 12022639 |
| chr12 | *ETV6* | 12022749 | 12023009 |
| chr12 | *ETV6* | 12043767 | 12043994 |
| chr12 | *KRAS* | 25378535 | 25378795 |
| chr12 | *KRAS* | 25380238 | 25380478 |
| chr12 | *KRAS* | 25398227 | 25398433 |
| chr12 | *SH2B3* | 111884535 | 111884777 |
| chr12 | *SH2B3* | 111884791 | 111885049 |
| chr12 | *SH2B3* | 111885214 | 111885424 |
| chr12 | *PTPN11* | 112884014 | 112884254 |
| chr12 | *PTPN11* | 112888115 | 112888350 |
| chr12 | *PTPN11* | 112893742 | 112893975 |
| chr12 | *PTPN11* | 112915377 | 112915582 |
| chr12 | *PTPN11* | 112926203 | 112926424 |
| chr12 | *PTPN11* | 112926824 | 112927050 |
| chr12 | *PTPN11* | 112942491 | 112942728 |
| chr13 | *FLT3* | 28578139 | 28578348 |
| chr13 | *FLT3* | 28588513 | 28588753 |
| chr13 | *FLT3* | 28589224 | 28589443 |
| chr13 | *FLT3* | 28589621 | 28589866 |
| chr13 | *FLT3* | 28592473 | 28592726 |
| chr13 | *FLT3* | 28597387 | 28597639 |
| chr13 | *FLT3* | 28598932 | 28599132 |
| chr13 | *FLT3* | 28601175 | 28601423 |
| chr13 | *FLT3* | 28602289 | 28602513 |
| chr13 | *FLT3* | 28607933 | 28608152 |
| chr13 | *FLT3* | 28608168 | 28608392 |
| chr13 | *FLT3* | 28608392 | 28608635 |
| chr13 | *FLT3* | 28609600 | 28609850 |

| | | | |
|---|---|---|---|
| chr13 | *FLT3* | 28610014 | 28610260 |
| chr13 | *FLT3* | 28611230 | 28611480 |
| chr13 | *FLT3* | 28622379 | 28622629 |
| chr13 | *FLT3* | 28623491 | 28623741 |
| chr13 | *FLT3* | 28623743 | 28623993 |
| chr13 | *FLT3* | 28624191 | 28624429 |
| chr13 | *FLT3* | 28626645 | 28626890 |
| chr13 | *FLT3* | 28631453 | 28631699 |
| chr13 | *FLT3* | 28635981 | 28636231 |
| chr13 | *FLT3* | 28644552 | 28644798 |
| chr15 | *MAP2K1* | 66727349 | 66727596 |
| chr15 | *MAP2K1* | 66728980 | 66729220 |
| chr15 | *MAP2K1* | 66735593 | 66735803 |
| chr15 | *MAP2K1* | 66774053 | 66774267 |
| chr15 | *MAP2K1* | 66782741 | 66782973 |
| chr15 | *IDH2* | 90631740 | 90631990 |
| chr16 | *CREBBP* | 3779649 | 3779892 |
| chr16 | *CREBBP* | 3823590 | 3823830 |
| chr16 | *CREBBP* | 3832666 | 3832910 |
| chr16 | *MAPK3* | 30128455 | 30128688 |
| chr16 | *MAPK3* | 30129372 | 30129626 |
| chr16 | *SRCAP* | 30718974 | 30719219 |
| chr16 | *SRCAP* | 30723827 | 30724067 |
| chr17 | *TP53* | 7572897 | 7573129 |
| chr17 | *TP53* | 7577071 | 7577315 |
| chr17 | *TP53* | 7577397 | 7577636 |
| chr17 | *TP53* | 7578075 | 7578315 |
| chr17 | *TP53* | 7578363 | 7578623 |
| chr17 | *TP53* | 7579501 | 7579761 |
| chr17 | *NF1* | 29508376 | 29508636 |
| chr17 | *NF1* | 29527958 | 29528193 |
| chr17 | *NF1* | 29533184 | 29533424 |
| chr17 | *NF1* | 29553440 | 29553700 |
| chr17 | *NF1* | 29562707 | 29562943 |
| chr17 | *NF1* | 29667507 | 29667736 |
| chr17 | *NF1* | 29683941 | 29684174 |
| chr17 | *STAT5B* | 40354363 | 40354581 |
| chr17 | *STAT5B* | 40354621 | 40354863 |
| chr17 | *STAT5B* | 40359626 | 40359871 |
| chr17 | *STAT5B* | 40370757 | 40371014 |
| chr17 | *STAT5A* | 40452653 | 40452905 |
| chr17 | *STAT5A* | 40460083 | 40460306 |
| chr17 | *STAT5A* | 40461369 | 40461629 |

| | | | |
|---|---|---|---|
| chr17 | *STAT3* | 40469205 | 40469425 |
| chr17 | *STAT3* | 40474337 | 40474543 |
| chr17 | *STAT3* | 40475017 | 40475260 |
| chr18 | *SETBP1* | 42531847 | 42532089 |
| chr19 | *MAP2K2* | 4101010 | 4101267 |
| chr19 | *MAP2K2* | 4102235 | 4102485 |
| chr19 | *MAP2K2* | 4110520 | 4110769 |
| chr19 | *MAP2K2* | 4117506 | 4117766 |
| chr19 | *JAK3* | 17943190 | 17943409 |
| chr19 | *JAK3* | 17945519 | 17945768 |
| chr19 | *JAK3* | 17945926 | 17946185 |
| chr19 | *JAK3* | 17947979 | 17948219 |
| chr19 | *JAK3* | 17954120 | 17954371 |
| chr19 | *CEBPA* | 33792253 | 33792503 |
| chr19 | *CEBPA* | 33793090 | 33793338 |
| chr19 | *RRAS* | 50140143 | 50140413 |
| chr19 | *CD33* | 51728357 | 51728615 |
| chr2 | *DNMT3A* | 25457050 | 25457294 |
| chr2 | *DNMT3A* | 25458480 | 25458718 |
| chr2 | *DNMT3A* | 25463106 | 25463346 |
| chr2 | *DNMT3A* | 25463493 | 25463717 |
| chr2 | *DNMT3A* | 25467415 | 25467632 |
| chr2 | *ASXL2* | 25966895 | 25967154 |
| chr2 | *ASXL2* | 25972624 | 25972869 |
| chr2 | *ASXL2* | 25973036 | 25973241 |
| chr2 | *SOS1* | 39249824 | 39250056 |
| chr2 | *SF3B1* | 198266698 | 198266913 |
| chr2 | *SF3B1* | 198267323 | 198267549 |
| chr2 | *IDH1* | 209113085 | 209113297 |
| chr20 | *ASXL1* | 31017032 | 31017239 |
| chr20 | *ASXL1* | 31020968 | 31021193 |
| chr20 | *ASXL1* | 31022168 | 31022417 |
| chr20 | *ASXL1* | 31022567 | 31022827 |
| chr20 | *ASXL1* | 31022965 | 31023205 |
| chr21 | *RUNX1* | 36231692 | 36231937 |
| chr21 | *RUNX1* | 36252819 | 36253046 |
| chr21 | *U2AF1* | 44514752 | 44514997 |
| chr21 | *U2AF1* | 44524416 | 44524634 |
| chr22 | *MAPK1* | 22127115 | 22127325 |
| chr22 | *MAPK1* | 22142917 | 22143157 |
| chr22 | *MAPK1* | 22153310 | 22153534 |
| chr22 | *MAPK1* | 22160227 | 22160456 |
| chr22 | *MAPK1* | 22161969 | 22162197 |

| | | | |
|---|---|---|---|
| chr22 | *MAPK1* | 22221427 | 22221652 |
| chr22 | *EP300* | 41553275 | 41553494 |
| chr22 | *EP300* | 41556594 | 41556831 |
| chr22 | *EP300* | 41574208 | 41574447 |
| chr3 | *SETD2* | 47058395 | 47058633 |
| chr3 | *EP300* | 47103646 | 47103860 |
| chr3 | *GATA2* | 128200077 | 128200327 |
| chr3 | *GATA2* | 128200668 | 128200928 |
| chr3 | *GATA2* | 128202699 | 128202899 |
| chr3 | *PIK3CB* | 138374149 | 138374377 |
| chr3 | *PIK3CB* | 138376488 | 138376696 |
| chr3 | *PIK3CB* | 138409904 | 138410124 |
| chr3 | *PIK3CB* | 138417747 | 138417988 |
| chr3 | *PIK3CB* | 138426083 | 138426336 |
| chr3 | *PIK3CA* | 178916781 | 178916981 |
| chr3 | *PIK3CA* | 178917420 | 178917667 |
| chr3 | *PIK3CA* | 178921356 | 178921603 |
| chr3 | *PIK3CA* | 178922173 | 178922395 |
| chr3 | *PIK3CA* | 178927282 | 178927490 |
| chr3 | *PIK3CA* | 178927903 | 178928119 |
| chr3 | *PIK3CA* | 178936054 | 178936314 |
| chr3 | *PIK3CA* | 178938890 | 178939112 |
| chr3 | *PIK3CA* | 178947706 | 178947918 |
| chr3 | *PIK3CA* | 178948011 | 178948270 |
| chr3 | *PIK3CA* | 178951922 | 178952192 |
| chr4 | *KIT* | 55589655 | 55589878 |
| chr4 | *KIT* | 55593574 | 55593801 |
| chr4 | *KIT* | 55599270 | 55599486 |
| chr4 | *TET2* | 106156708 | 106156920 |
| chr4 | *TET2* | 106157091 | 106157322 |
| chr4 | *TET2* | 106157488 | 106157694 |
| chr4 | *TET2* | 106157812 | 106158034 |
| chr4 | *TET2* | 106180623 | 106180844 |
| chr4 | *TET2* | 106193715 | 106193955 |
| chr4 | *TET2* | 106196119 | 106196359 |
| chr4 | *TET2* | 106196888 | 106197127 |
| chr4 | *TET2* | 106197190 | 106197405 |
| chr4 | *FAT1* | 187517634 | 187517877 |
| chr4 | *FAT1* | 187524540 | 187524773 |
| chr4 | *FAT1* | 187532681 | 187532911 |
| chr4 | *FAT1* | 187535375 | 187535615 |
| chr4 | *FAT1* | 187541581 | 187541820 |
| chr4 | *FAT1* | 187541862 | 187542102 |

| | | | |
|---|---|---|---|
| chr4 | *FAT1* | 187629158 | 187629398 |
| chr4 | *FAT1* | 187629962 | 187630201 |
| chr4 | *FAT1* | 187630314 | 187630542 |
| chr5 | *APC* | 112154882 | 112155088 |
| chr5 | *APC* | 112179777 | 112180031 |
| chr5 | *NPM1* | 170832233 | 170832491 |
| chr5 | *NPM1* | 170834648 | 170834851 |
| chr5 | *NPM1* | 170837462 | 170837704 |
| chr6 | *CCND3* | 41905055 | 41905274 |
| chr7 | *ABCA13* | 48411827 | 48412060 |
| chr7 | *IKZF1* | 50450114 | 50450357 |
| chr7 | *PIK3CG* | 106508471 | 106508724 |
| chr7 | *PIK3CG* | 106508781 | 106509041 |
| chr7 | *PIK3CG* | 106509241 | 106509486 |
| chr7 | *PIK3CG* | 106509515 | 106509775 |
| chr7 | *PIK3CG* | 106512941 | 106513176 |
| chr7 | *PIK3CG* | 106523396 | 106523615 |
| chr7 | *BRAF* | 140434357 | 140434573 |
| chr7 | *BRAF* | 140453059 | 140453266 |
| chr7 | *BRAF* | 140477761 | 140477983 |
| chr7 | *BRAF* | 140481366 | 140481601 |
| chr7 | *BRAF* | 140487266 | 140487476 |
| chr7 | *BRAF* | 140501240 | 140501441 |
| chr7 | *EZH2* | 148504738 | 148504978 |
| chr7 | *EZH2* | 148506372 | 148506589 |
| chr7 | *EZH2* | 148507406 | 148507618 |
| chr7 | *EZH2* | 148511032 | 148511276 |
| chr7 | *EZH2* | 148514917 | 148515124 |
| chr7 | *EZH2* | 148523481 | 148523726 |
| chr7 | *EZH2* | 148525653 | 148525888 |
| chr7 | *EZH2* | 148526737 | 148526948 |
| chr8 | *RAD21* | 117859853 | 117860065 |
| chr8 | *RAD21* | 117875360 | 117875610 |
| chr8 | *RAD21* | 117878806 | 117879014 |
| chr8 | *MYC* | 128750640 | 128750887 |
| chr8 | *MYC* | 128751169 | 128751429 |
| chr8 | *MYC* | 128752604 | 128752810 |
| chr9 | *JAK2* | 5073698 | 5073902 |
| chr9 | *JAK2* | 5078303 | 5078518 |
| chr9 | *JAK2* | 5089672 | 5089888 |
| chrX | *ZRSR2* | 15827260 | 15827494 |
| chrX | *ZRSR2* | 15833847 | 15834083 |
| chrX | *ZRSR2* | 15841187 | 15841437 |

| | | | |
|---|---|---|---|
| chrX | *BCOR* | 39911356 | 39911576 |
| chrX | *BCOR* | 39922077 | 39922301 |
| chrX | *BCOR* | 39931984 | 39932228 |
| chrX | *BCOR* | 39933343 | 39933549 |
| chrX | *BCOR* | 39933743 | 39934001 |
| chrX | *BCOR* | 39934038 | 39934256 |
| chrX | *STAG2* | 123171369 | 123171576 |
| chrX | *STAG2* | 123176321 | 123176536 |
| chrX | *STAG2* | 123179153 | 123179393 |
| chrX | *STAG2* | 123181213 | 123181443 |
| chrX | *STAG2* | 123197003 | 123197263 |
| chrX | *STAG2* | 123215277 | 123215534 |
| chrX | *STAG2* | 123220412 | 123220633 |
| chrX | *PHF6* | 133527460 | 133527667 |
| chrX | *PHF6* | 133547448 | 133547683 |
| chrX | *PHF6* | 133549065 | 133549325 |
| chrX | *PHF6* | 133551195 | 133551417 |

## Supplemental Figure Legends

**Supplemental Figure 1.** Photomicrographs were taken of patient diagnostic samples. *Panel A* Bone marrow biopsy of UPN3160 showing myeloid hyperplasia (mature and precursors), scattered eosinophils, and few megakaryocytes. *Panel B* Bone marrow aspirate of UPN2861 showing numerous monocytic cells, several neutrophilic cells, and a nucleated red blood cells. *Panel C* Peripheral blood smear of UPN3426 showing mixture of cell types including neutrophil, monocytes, eosinophil precursor, nucleated red blood cell, and blast. *Panel D* Bone marrow aspirate of UPN3426 showing left-shifted granulocyte precursors, increased monocytes, few blasts, and few lymphocytes. *Panel E* Peripheral blood smear of patient UPN3436 showing mixture of cell types including neutrophils (including hypogranular forms), monocytes, eosinophils, basophil, lymphocyte, and nucleated red blood cell. *Panel F* Bone marrow aspirate of UPN3436 showing left-shifted granulocyte precursors, monocytes, few

blasts, few nucleated red >blood cells, and a portion of a megakaryocyte (lower left). (A: 40X objective, Hematoxylin & Eosin. B – F: 100X objective, Wright-Giemsa.)

**Supplemental Figure 2.** Sanger sequencing confirms germline configuration of *SH2B3* mutations in UPN1744 (left) and UPN3436 (right).

**Supplemental Figure 3.** *Panel A* Mutant iPSC-derived HPC but not wildtype HPC show spontaneous proliferation independent of GM-CSF, a hallmark of JMML. *Panel B* Immunoblotting of single and double mutant HPC showed elevated STAT5 and ERK signaling compared to WT HPC.

**Supplemental Figure 4.** Circos plot highlighting the association of *SH2B3* and *PTPN11* alterations. All but one patient with germline SH2B3 (g_SH2B3) mutation had no additional alterations, while patients with somatic *SH2B3* (s_SH2B3) mutations as well as *SH2B3* mutations of unknown configuration (u_SH2B3) frequently carried additional mutations in *PTPN11* compared to other Ras/MAPK signaling genes.

**Supplemental References**


1. Mills JA, Paluru P, Weiss MJ, Gadue P, French DL. Hematopoietic Differentiation of Pluripotent Stem Cells in Culturee. In: Methods in Molecular Biology, vol. 1185. 2014. p181–194.
2. Demaree B, Delley CL, Vasudevan HN, et al. Joint profiling of DNA and proteins in single cells to dissect genotype-phenotype associations in leukemia. Nat Commun 2021;12(1):1583.
3. Pellegrino M, Sciambi A, Treusch S, et al. High-throughput single-cell DNA sequencing of acute myeloid leukemia tumors with droplet microfluidics.

Genome Res 2018;28(9):1345–1352.

4. DePristo MA, Banks E, Poplin R, et al. A framework for variation discovery and genotyping using next-generation DNA sequencing data. Nat Genet 2011;43(5):491–498.

5. Landrum MJ, Lee JM, Benson M, et al. ClinVar: improving access to variant interpretations and supporting evidence. Nucleic Acids Res 2018;46(D1):D1062–D1067.

6. Tate JG, Bamford S, Jubb HC, et al. COSMIC: the Catalogue Of Somatic Mutations In Cancer. Nucleic Acids Res 2019;47(D1):D941–D947.

7. Miles LA, Bowman RL, Merlinsky TR, et al. Single-cell mutation analysis of clonal evolution in myeloid malignancies. Nature 2020;587(7834):477–482.

8. Morita K, Wang F, Jahn K, et al. Clonal evolution of acute myeloid leukemia revealed by high-throughput single-cell genomics. Nat Commun 2020;11(1):5327.

9. Jahn K, Kuipers J, Beerenwinkel N. Tree inference for single-cell data. Genome Biol 2016;1786.

10. Mulè MP, Martins AJ, Tsang JS. Normalizing and denoising protein expression data from droplet-based single cell profiling. Nat Commun 2022;13(1):2099.

11. Stieglitz E, Taylor-Weiner AN, Chang TY, et al. The Genomic Landscape of Juvenile Myelomonocytic Leukemia. Nat Genet 2015;47(11):1326–1333.

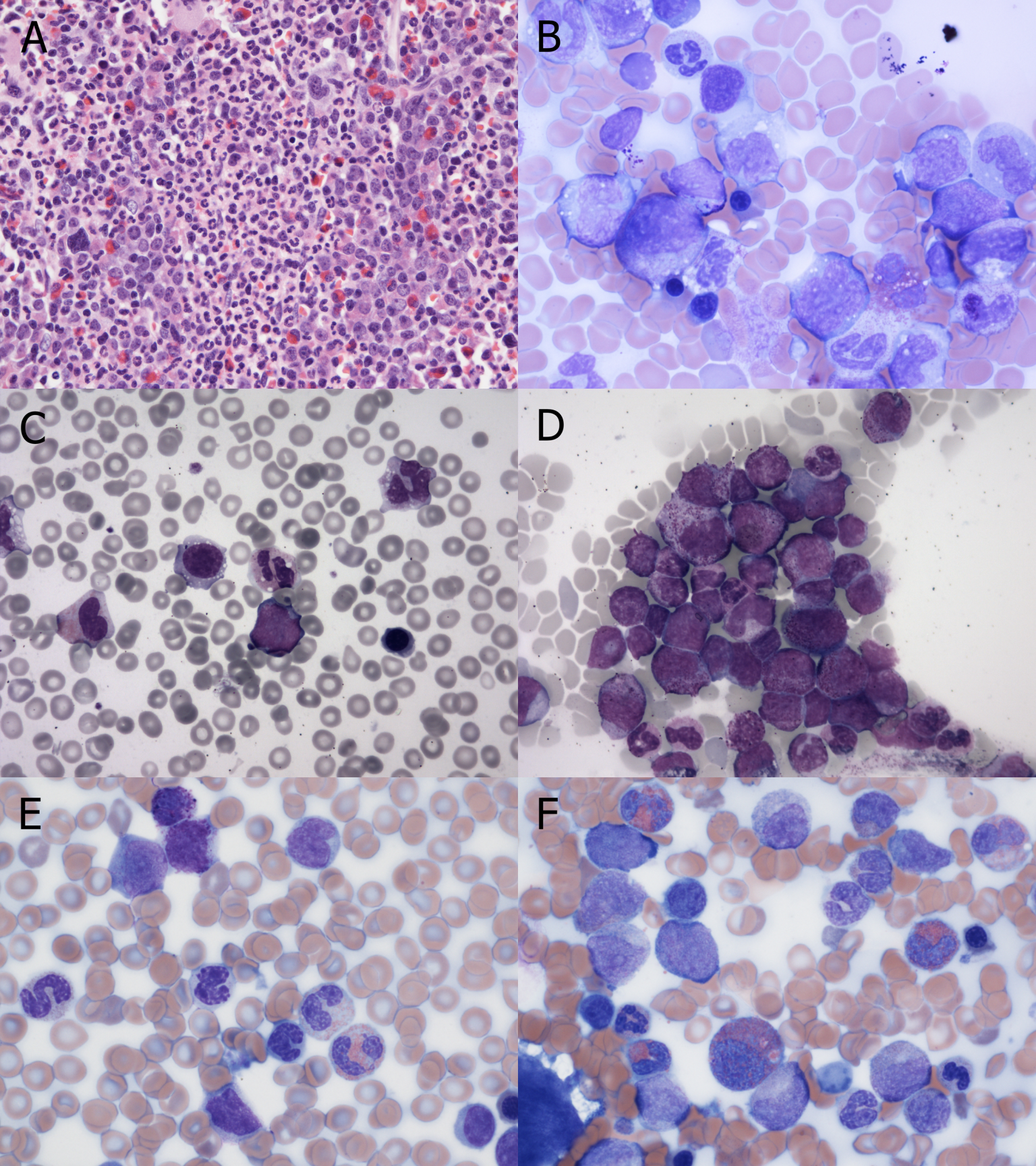
A
B
C
D
E
F

## UPN1744

Sorted CD3+ T cell sample

c.751C>T

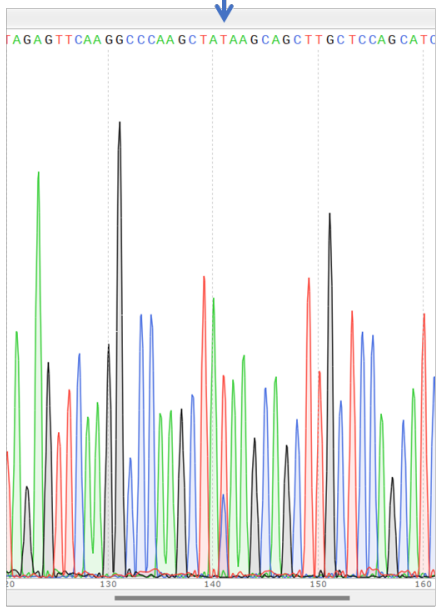

Diagnosis sample

c.751C>T

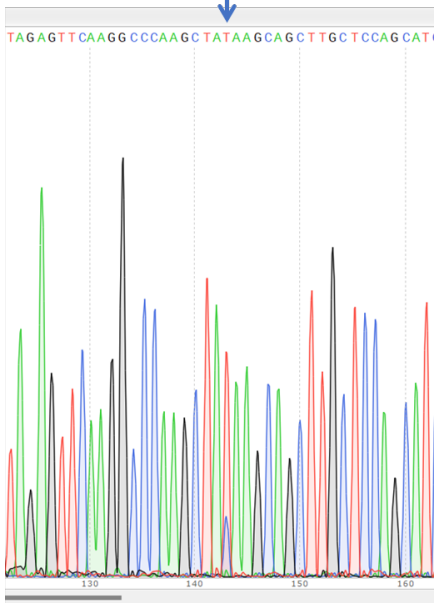

## UPN3436

Buccal sample

c.1175G>A

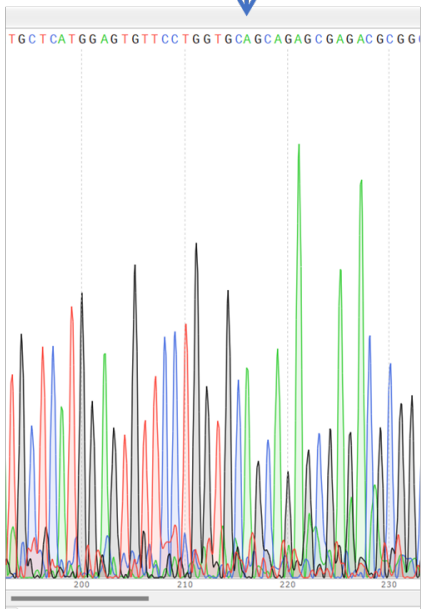

Diagnosis sample

c.1175G>A

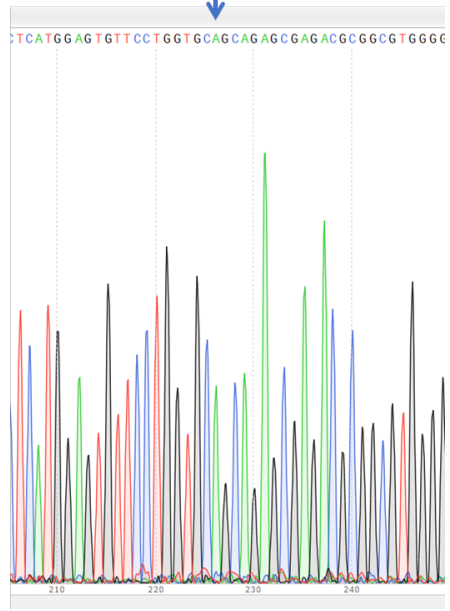

**A**

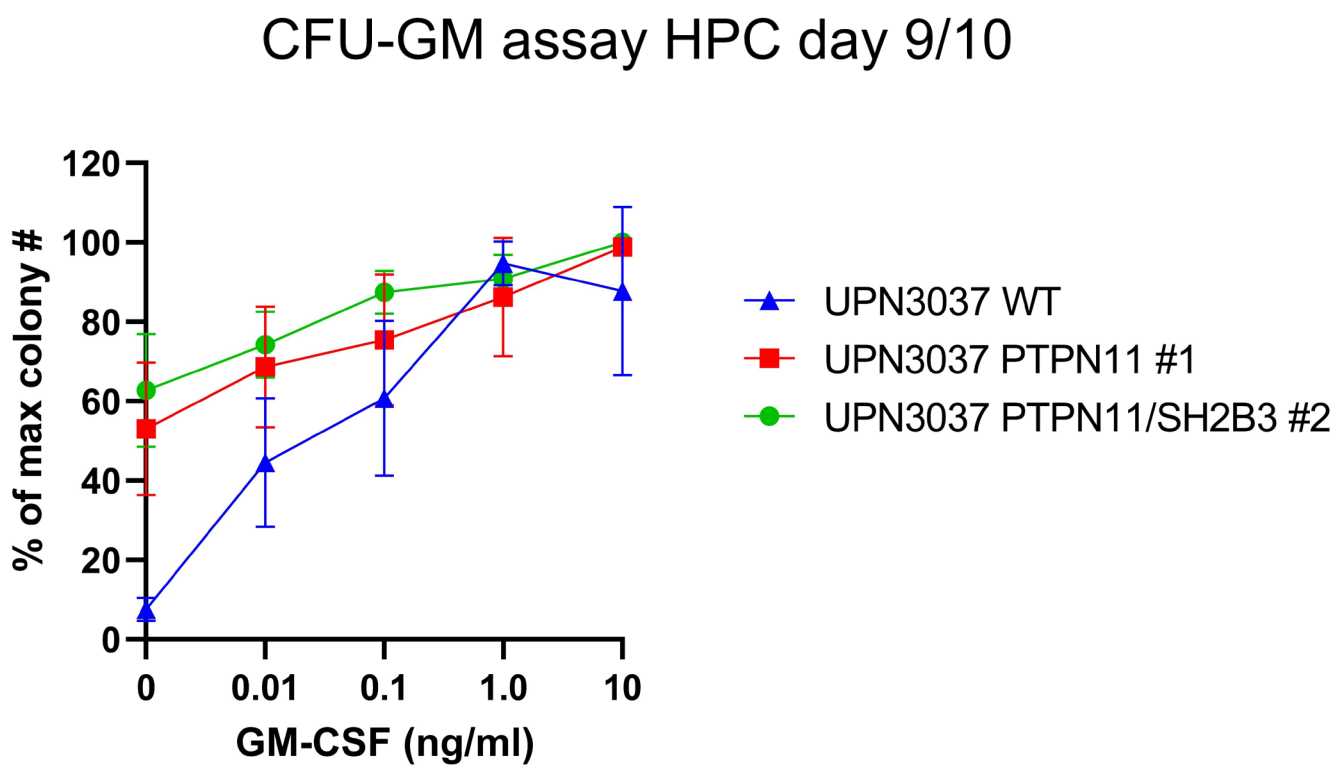
CFU-GM assay HPC day 9/10
% of max colony #
120
100
80
60
40
20
0
0
0.01
0.1
1.0
10
GM-CSF (ng/ml)
UPN3037 WT
UPN3037 PTPN11 #1
UPN3037 PTPN11/SH2B3 #2

**B**

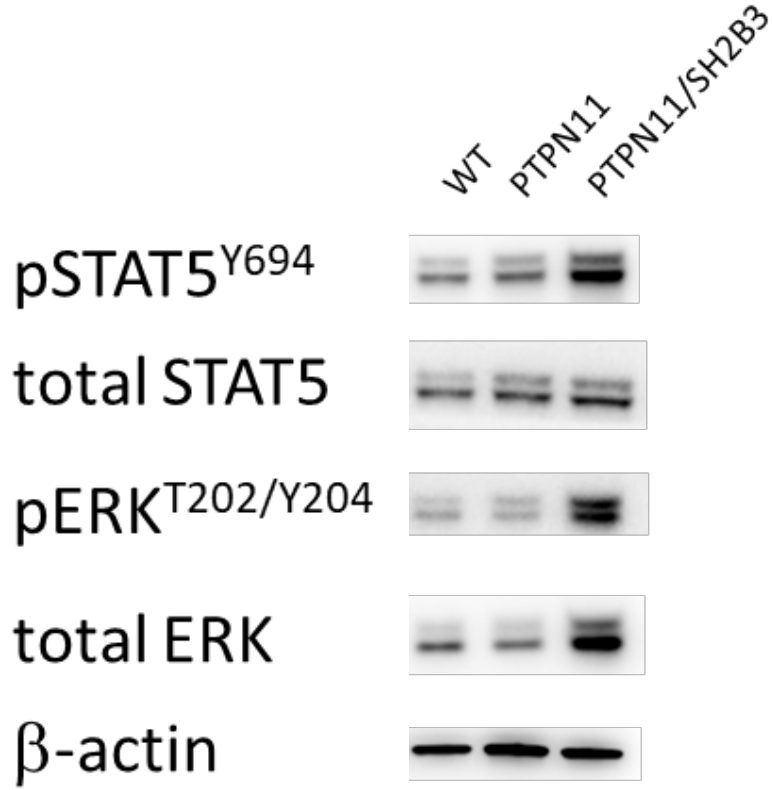
WT
PTPN11
PTPN11/SH2B3
pSTAT5Y694
total STAT5
pERKT202/Y204
total ERK
β-actin

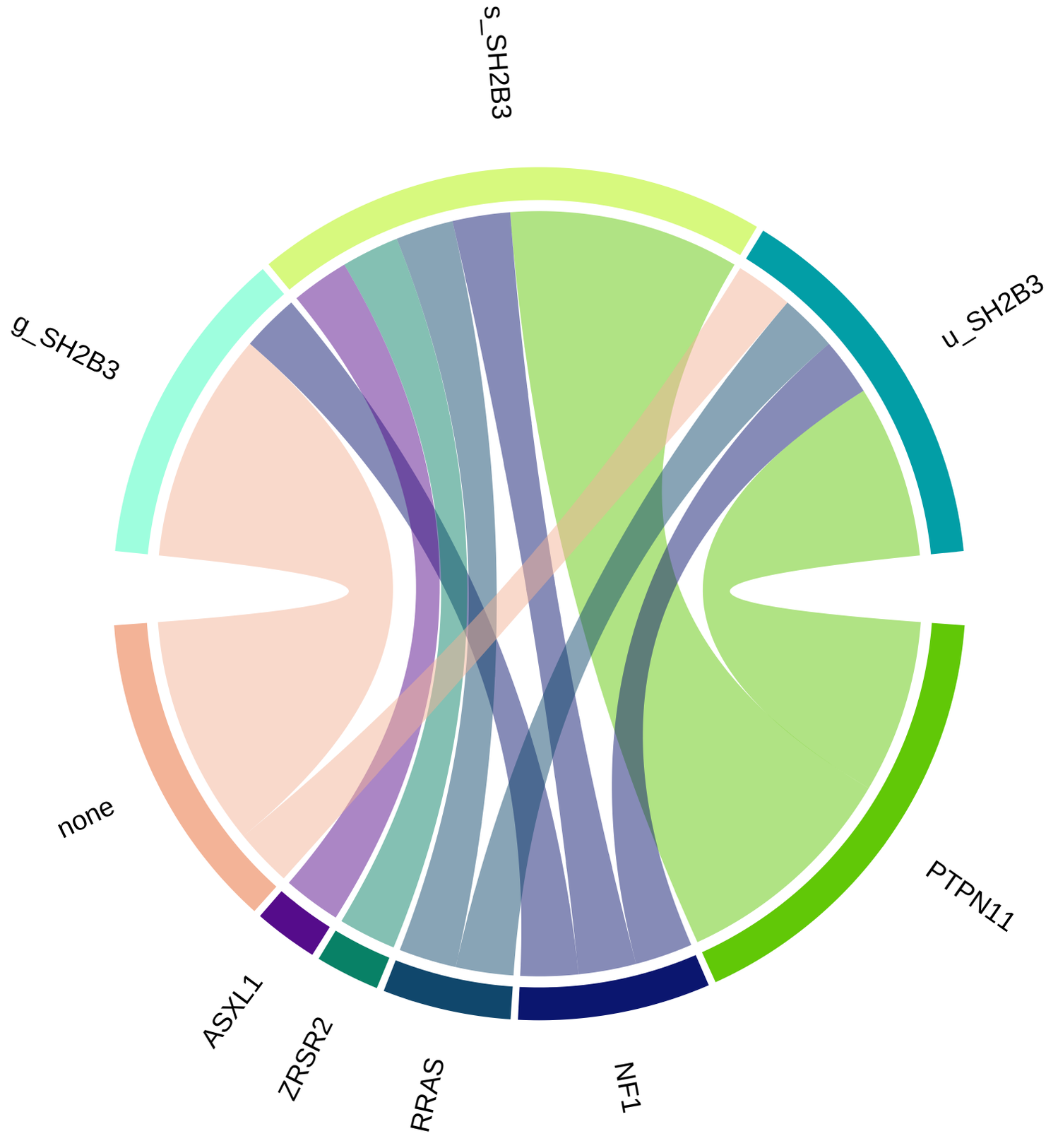
s_SH2B3
u_SH2B3
PTPN11
NF1
RRAS
ZRSR2
ASXL1
none
g_SH2B3